

The diurnal cycle of cloud profiles over land and ocean between 51°S and 51°N, seen by the CATS spaceborne lidar from the International Space Station

Vincent Noel ¹, H  l  ne Chepfer ², Marjolaine Chiriaco ³, John Yorks

Reply to Reviewers

June 19th, 2018

Original reviewer comments are in blue italics, our replies in black.

Reviewer 1 comments and replies

This is a review of “The diurnal cycle of cloud profiles over land and ocean between 51°S and 51°N, seen by the CATS spaceborne lidar from the International Space Station”

This paper presents the cloud detection statistics from the CATS lidar that was operating on the ISS. Because of the non-sun-synchronous orbit of the ISS, these statistics sample all hours of day and night. This creates a unique dataset. This data is presented very well in the paper. I believe this is an excellent paper that will be cited a lot. I certainly recommend publication of the paper in ACP. There are a few minor issues that I recommend the authors to consider. Those are discussed below.

Like any lidar, CATS probes the first ~3 optical depths of a cloud, as discussed in the paper. In the case of thin cirrus clouds, the full extent of the clouds will be sampled, but in many cases essentially only the top height will be detected. However, the authors confuse this sampled vertical cloud fraction with statistics of vertical extent. For example, the abstract states “the high clouds geometric thickness increases significantly from 1km near 5PM to 5km near 10PM”. However, it could also be that the cloud top altitude is more variable later in the day, while the geometrical thickness is staying the same. The data could be analyzed in other ways to include transparent clouds only, which will allow a study of statistics of geometric thickness, but this is not done in the current study. I am not asking to change the study to include this analysis, but the authors should discuss the fact that real geometric extent is not always sampled here. Especially in the tropics a substantial part of the high clouds would be tops of convection that may have vary throughout the day. Other parts of the paper that refer to geometric thickness of clouds are at lines 340-344, 444, 492, 629, 636, and 642. There may be other instances. Please go through the paper and discuss this interpretation of the data correctly.

This interpretation is correct, and we thank the reviewer for pointing out this problem. We went through the paper (thanks for the pointers) and now try to present the reader a more correct interpretation of the results.

Line 172: If I understand correctly, lidar depolarization information is used for cloud classification. If so please briefly discuss this in the paper.

A sentence has been added to the CATS overview paragraph that briefly outlines the CATS cloud phase algorithm and references the appropriate papers for more details. The full description of the CATS cloud phase algorithm is presented in Section 4.3 of the CATS ATBD [1] and in an AMT paper soon to be submitted. High confidence liquid water clouds are classified if the cloud layer has a $T_{mid} > 0$ C and high confidence ice clouds are identified as cloud layers with a $T_{mid} < -20$ C. These ice clouds and liquid water clouds are assigned a CP score of 10 and -10, respectively. Next, the CP algorithm identifies high confidence ice cloud layers as those layers with 1064 nm depolarization ratios greater than 0.25 or $T_{mid} < -10$ C (CP Score = 9). High confidence liquid water clouds are classified if the cloud layer has a 1064 nm depolarization ratio < 0.15 (CP Score = -9). The remaining layers are determined to have lower confidence cloud phase and are assigned a CP Score with an absolute value of 7 or less. These thresholds are based on Yorks et al. (2011) and Hu et al. (2009). Comparisons

with CALIOP have shown very good agreement between the two instruments for cloud phase.

[1] https://cats.gsfc.nasa.gov/media/docs/CATS_ATBD_V1-02.pdf

Line 372: It seems that a reference to Johnson et al. (1999; J. Climate, 12, 2397–2418) about the tri-modal nature of tropical convection is in place here.

We thank the reviewer for this very useful reference and comment, which are now both included in the text. Note however that CATS only reports a significant population of those midlevel clouds (5-7km) over land, and not over ocean. This is not consistent with those clouds being cumulus congestus, as these also appear over ocean (Masugana et al. 2005). Higher-altitude clouds, which cloud mask such clouds from the lidar view, are equally frequent over ocean and land, so this inconsistency is not explained by instrumental bias.

Following the references provided by Reviewer 2 suggests those clouds could be Altocumulus, as both share middle-level altitudes and locations over land in the summer hemisphere. This possibility is also now mentioned in the text.

Line 515: Another thing to note is that, besides cloud detection, retrieving a cloud top height from passive instruments is not as straightforward as it is for lidar measurements, especially for thin clouds and in multi-layered situations.

We agree with the reviewer and have modified the text to include this point.

Figure 5 (and A7): I would suggest to add a vertical scale to the Africa-North plot, or maybe to all of the plots.

Following this comment, we have added vertical scales to all the subplots of Figures 5 and A7.

Figure 6: Because of the ISS orbit, CATS samples between 51 degrees north and south, as explained in the paper. However, figure 6 and the discussion are not consistent with this geographical limitation and include statistics supposedly from latitude bands of 30-60 degrees north and south. This choice is made to be consistent with previous studies, but hides the fact that CATS is only sampling to 51 degrees, making the data not completely consistent with previous datasets. It is important to be consistent about the sampling region throughout the paper. Also, I find the labels of the latitude bands on the right side of figure 6 rather confusing. It makes it seem like vertical axis are latitudes in addition to cloud amount deviation somehow. I would propose adding the latitude bands on top or inside the figure as a label or legend.

We agree with the reviewer's position, and have updated figure 6 to be hopefully less confusing, and convey the actual sampling latitude range of CATS.

Reviewer 2 comments and replies

Review "The diurnal cycle of cloud profiles over land and ocean between 51°S and 51°N, seen by the CATS spaceborne lidar from the International Space Station" by Noel et al.

By using CATS measurement, the paper presents a first land-ocean contrast of cloud diurnal cycle. Results are very useful. However, there are many uncertainties associated with CATS data for diurnal cloud studies, which need to be clearly discussed. I suggest the paper for publication after the following comments are properly addressed.

Major issues

1. There are many challenges in using CATS data to study diurnal cloud cycle. First, it is linked with space lidar observations itself. Although several points (day-night solar background difference, attenuation of lidar signal by upper and middle clouds) are touched in the paper, they are needed to be clearly presented and quantified. Results discussions need to consider these uncertainties.

The paper now includes more extensive comparisons with ground-based datasets, that we hope will help the reader understand the strengths and limitations of spaceborne lidar measurements, including the influence of attenuation by upper and middle clouds on the detected low-altitude clouds.

Regarding the day-night variation, the CATS minimum detectable backscatter (MDB) at 1064nm goes from $5.10 \cdot 10^{-5} \text{ km}^{-1} \text{ sr}^{-1}$ in absence of sunlight to $1.30 \cdot 10^{-3} \text{ km}^{-1} \text{ sr}^{-1}$ in illuminated conditions (Yorks et al., 2016). CATS daytime profiles are horizontally averaged across 60km before cloud detection, which bring the daytime MDB down to nighttime levels. This has two implications for daytime data: 1) optically thinnest clouds detected during nighttime at 60km horizontal averaging might be absent from daytime detections, these represent roughly ~5% of nighttime clouds. 2) cloud amounts might be overestimated when many clouds with small horizontal extent are present - this mainly concerns boundary layer clouds. In our evaluations, the associated decrease in SNR due to solar background has a bigger impact on aerosol layer detection than clouds.

CATS's MDB is smaller than CALIOP's 532nm daytime MDB ($1.70 \cdot 10^{-3} \text{ km}^{-1} \text{ sr}^{-1}$), so all other things being equal CATS should detect more clouds than CALIOP in daytime conditions. Both Sassen et al. (2009) and Gupta et al. (2018) successfully used CALIPSO cloud detections in both nighttime and (solar-affected) daytime conditions to document part of the diurnal variability of clouds and, like us, report more high clouds in nighttime measurements. They remark that the observed nighttime increase is considerably more than the uncertainty that might arise from the daytime loss of detection sensitivity. Since CATS cloud detection abilities are at least on par with CALIOP's in daytime conditions, and CALIOP daytime detections are found acceptable to document part of the diurnal cycle, it follows that the existence of solar pollution in the CATS dataset should not prevent its use to document the

diurnal cycle of clouds. As in the Sassen and Gupta papers, we note that how much CALIPSO (and therefore CATS) daytime detections underestimate high clouds occurrence and overestimate low clouds need to be quantified.

These points are now made in the text (Sect. 2.1, 3.1 and 5).

In a similar way, how extinction from high clouds affects the retrieval of low-level clouds remains unquantified and hard to evaluate for all spaceborne lidars. Comparisons with ground-based datasets (see major point 3) suggest that high clouds do not impair significantly the retrieval of low clouds over any site. Over ARM-ENA (oceanic site), the limited amount of high clouds means CATS reports of low clouds amounts is very close to the ground-based one. Over ARM-SGP the relatively large amount of high clouds at night might explain why CATS misses half of the nighttime low and mid-level clouds observed by the ground radar. Supposing that 50% of unsampled profiles due to masking by high clouds are indeed cloudy (i.e. an hypothesis of random overlap) is not sufficient to fix the space-ground disagreement. We think extending these results to the global scale for CATS (and CALIPSO) would be a interesting future project.

The upcoming paper by Yorks et al. (In preparation for AMT) will quantify these points further. We have tried to discuss the importance of uncertainties on the results presented here in the last section of the article.

2. It needs to be very clear that CATS from ISS don't provide exact diurnal cycle cloud observations as ground-based observations. Due to the nature of ISS orbit characters, you need to combine over a month-long measurements together to cover the diurnal cycle. So, composed the diurnal cycle include seasonal cloud variations. Although it is fine to perform the seasonal study as discussed in the paper, it is important to make readers aware of the nature of CATS diurnal cloud properties. Thus, related information needs to be added in the introduction or the method section.

Following this comment, we have updated the introduction (before-last paragraph) to make clear 1) that the CATS lidar cannot track the evolution of cloudiness above a particular location along a particular day and 2) that we recreate the cloud diurnal cycle over a given location by aggregating over seasons the cloud detections made by CATS over that particular location at different times of day. We now make this point again in the relevant Data and Methods section (Sect. 2.2.a, 2nd paragraph).

3. One way to make these limitations well understood is by using ground-based observations to validate CATS results. Although there is one figure for this purpose, it is not enough. Tropical observations and over oceans are needed. ARM observations are available for the validations.

Following this comment, and major comment #2 from Reviewer 3, we have tried locating a

well-documented, 24/24 dataset of cloud layers covering the period 2015-2017 based on measurements from a ground-based lidar operating in the Tropics, preferably close to the ocean. We have contacted several observatories (e.g OPAR) but it appears lidar-based cloud layer products are often unvalidated and/or suffer from irregular or non-diurnal sampling.

Following the Reviewer's suggestion, we investigated ARM data [1] and found several datasets based on Tropics measurements and promising cloud layer information. We found that:

- Datasets from Nauru Island and Darwin Australia did not overlap with CATS timeframe
- Datasets from Brazil and Ascension Island cover the CATS timeframe but only contained profiles of Attenuated Backscatter (without cloud detection) — doing the cloud detection ourselves would require external validation
- Only datasets from the ARM Eastern North Atlantic (ENA) atmospheric observatory [2] are close to our criterias above. This site provides cloud layers derived from ground-based lidar measurements made in an oceanic environment, unlike the SIRTA and ARM-SGP datasets considered in the initial article.

Since the ENA observatory is located at 39°N, it is at best sub-tropical. It is however the only oceanic ARM site we found that could provide a 24/24 robust dataset of cloud layers covering the CATS time period.

Our initial exploration of the enaarsclkazrbnd1kolliasC1 dataset (based on a combination of lidar and radar data) showed unusual results during the 2017 summer (see figure below). We contacted ARM people, who explained the problem comes from unresolved issues with lidar cloud detections and suggested rebuilding the cloud layers based on the cloud mask source product and ignoring the lidar-only detections. This resolved the problem, but in effect turned it into a radar-based product.

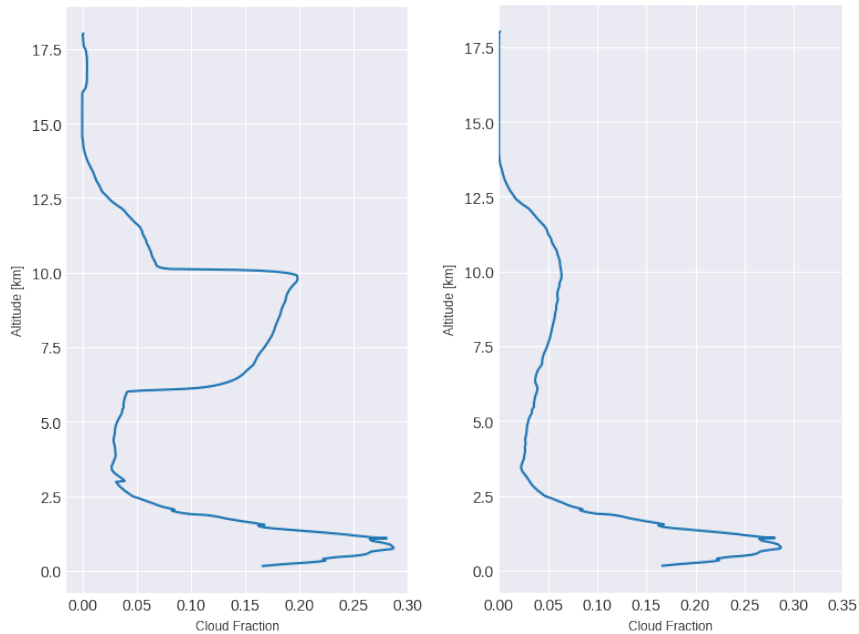


Figure 1 - Cloud fraction over ARM-ENA for 2017 JJA using both lidar and radar cloud detections (left) and radar-only cloud detections (right)

The paper now includes (Sect. 3.3) a direct comparison of the diurnal cycles of cloud fraction profiles as documented by CATS over the ENA site and from ground-based radar detections. We have also obtained the ARM-SGP ground-based lidar+radar cloud detections in order to directly include them in the paper for comparison with CATS data. Exploration of the `sgparsclkazrbnd1kolliasC1` dataset showed artefacts similar to those from the ARM-ENA datasets (vertical steps in cloud fraction) when including lidar-only cloud detections. We thus had again to consider only radar detections, leading to results very similar to those presented in Zhao et al. (2016).

The fact that we uncovered issues with those ARM datasets, which are apparently among the most reliable, confirms how difficult it is to obtain faultless lidar-based cloud retrievals over long periods. Providing our own analysis of the data allowed us to only use cloud detections made during the CATS operation period, making time periods consistent across all ground-based comparisons.

The article now includes comparisons between CATS and:

- Lidar-based cloud retrievals from a midlatitude continental site (SIRTA), already described in e.g. Noel et Haeffelin (2006)
- Radar-based cloud retrievals from a midlatitude continental site (ARM-SGP), already described in e.g. Zhao et al. (2016)
- Radar-based cloud retrivals from a subtropical oceanic site (ARM-ENA).

We hope these improvements to our comparisons between CATS and ground-based datasets better highlights the strenghts and limitations of spaceborne and ground-based lidar cloud

sampling.

[1] <https://www.arm.gov/data>

[2] <https://www.arm.gov/capabilities/observatories/ena>

Minor issues

1. L23-24: change "high clouds maximum" to "high cloud thickness maximum." The interpretation of cloud thickness detected by a lidar has to consider cloud optical thickness.

Following the first comment from reviewer 1, the text referenced here has been modified. We hope it now satisfies the concern expressed here.

2. Line 88-101: Some references are needed here to support the discussion. For example, the Fig. 9 of Wang and Sassen 2001, will support your middle latitude discussion.

Wang, Z., and K. Sassen, 2001: Cloud type and macrophysical property retrieval using multiple remote sensors. J. Appl. Meteor., 40, 1665-1682.

Our initial idea was that paragraph would sum up the findings of the articles referenced in the previous paragraph ("Those studies..."). However, the first paragraph only references studies of cloud diurnal cycles documented from space, whereas the findings in the second paragraph are general. Following this observation, we have revised the first two paragraphs of the introduction, trying to support our assertions with appropriate references, including the one suggested by the reviewer. We thank the reviewer for that very on-point reference.

This comment echoes Major Issue #1 from reviewer 3.

3. Line 106-107: There are many more important related papers should be cited than your paper.

We thank the reviewer for pointing this out. We have updated the manuscript to include references to papers that are hopefully more important.

4. L165: "measured every 350m" not accurate. It is a 350 m average profile.

The Reviewer is correct. CALIPSO sends every 1/20th of a second a laser pulse, which travels to the Earth's surface and back before the satellite has time to move significantly and thus can be considered instantaneous. Unlike CALIPSO, CATS has a high repetition rate of 5kHz and monitors constantly for backscattered energy. The onboard data system accumulates 250 of these 5kHz profiles and reports the data every $\pm 350\text{m}$ to approximate a 20Hz measurement rate.

The text has been changed to “CATS reports vertical profiles of Attenuated Total Backscatter (ATB) every 350m at 1064nm with a 60m vertical resolution (Yorks et al., 2016a). Each profile is created by accumulating backscattered energy from 250 5kHz pulses, 20 times per second.”

5. L 171: What is "L2O"?

Files for CATS level 2 layer products share the prefix "CATS-ISS_L2O_N-M7.2-V2-01_05kmLay". The L2O designation identifies “Level 2 Operational” products. The updated text now includes this explanation.

6. L201-202: So you shouldn't use this site considering it data collection biases.

Unfortunately, the number of site providing datasets containing 24-hour retrievals of cloud boundaries derived from active measurements and part of published research is currently limited, as we explained in our answer to major comment #3. Even lidar-based cloud retrievals from ARM sites suffer from artefacts that prevent their use in this study.

In the updated manuscript we now include, in addition to direct comparisons of CATS with SIRTA lidar retrievals (over midlatitude western Europe), comparisons of cloud retrievals from CATS with others based on measurements from ARM-ENA (subtropical oceanic) and ARM-SGP (midlatitude US) observation sites. As the ARM retrievals are radar-only, we decided to keep the SIRTA dataset as it is the only lidar-based ground-based cloud retrievals dataset.

7. L273-274, "low clouds have their base below 4km ASL": Do you sure that you mean cloud base height here. If so, it does not make sense. First, it is almost impossible for you to detect the base of optically thick clouds. Assuming that you can detect, we refer clouds with the base higher than 2 km as middle-level clouds. Using top height will make more sense.

The Reviewer is correct, the original sentence mixed up cloud base and top. Thanks for noticing that error. The text now includes the correct explanation: low clouds have their top below 4km ASL, high clouds have their base above 7km, and mid-level clouds are in between.

8. L308-308: Not necessarily true. How often do you detect low clouds below high clouds? Even if high cloud occurrences are high, they are not 100.

The reviewer is correct, the logic of the discussion was incorrect. We have modified the text to fix the discussion and hopefully better make the point we were trying to make.

9. L315-316: Solar-background variations need to be better quantified.

We addressed the solar background variations issue in our answer to major comment #1.

10. L336-346: To what extent, these variations are due to the lower daytime detection sensitivity, especially considering the contrast between N30-50 with S30-50?

We addressed the issue of solar background variations in our reply to major comment #1.

11. L368-374: The high occurrence of middle-level clouds are well documented by many early studies (Zhang et al. 2010; Sassen and Wang 2012, and other), which should be properly referenced.

Zhang, D., Z. Wang, and D. Liu (2010), A global view of midlevel liquid-layer topped stratiform cloud distribution and phase partition from CALIPSO and CloudSat measurements, J. Geophys. Res., 115, D00H13, doi:10.1029/2009JD012143.

Sassen, K. and Z. Wang, 2012: The Clouds of the Middle Troposphere: Composition, Radiative Impact, and Global Distribution, Surv Geophys (2012) 33:677-691, DOI 10.1007/s10712-011-9163-x

The mid-level clouds CATS detects over Africa, South America and Australia, in the North hemisphere in JJA and the South hemisphere in DJF, might very well be Altopcumulus clouds that Wang and Sassen (2012) document in the same locations, altitudes and times. This possibility is now discussed in the text. We thank the Reviewer for this useful reference.

12. L411-473: This part of the discussion should occur early in the paper as validation efforts.

We present the results at global scale first on purpose, as we consider those are the most novel and interesting for potential readers. Since validation efforts are not the main purpose of the paper, we think nothing is lost by delaying their presentation.

13. L421-422: Considering the night time sampling biases, I don't think that you can trust this result.

We have modified the text to include this observation.

14. L449-452: It will good to include a panel for SGP ground-based observation results here.

As noted before, for the revision we have obtained the ARM-SGP ground-based lidar+radar cloud detections from the ARM site. From those, we have extracted radar-only detections (to avoid bias from spurious lidar detections) and derived the daily cycle of vertical cloud fraction profiles during the CATS period (JJA 2015-2017). These results are now included in the paper's Figure 4. They are very similar to those presented in Zhao et al. (2016).

15. L484-487: In Fig. 5, why cloud top in Europe JJA is significantly lower than the other regions?

Europe is the only region in Fig. 5 that does not include part of the Tropical band, where the tropopause reaches much higher altitudes. This leads to cloud tops over Europe

We included this information in the legend of Figure 5 in the updated manuscript version that we submitted in March (this version has “over land and ocean” in the title), which superseded our original submission in February and became the one available from the ACPD website during the open discussion [1]. We do not know why the reviewers were provided with the non-updated version and regret the confusion.

[1] <https://www.atmos-chem-phys-discuss.net/acp-2018-214/acp-2018-214.pdf>

16. L522: Where is ISCCP data? Is there any reason not to plot it?

Indeed, we have decided against directly including retrievals based on ISCCP in the paper. By doing so, our goal is to prevent the discussion from focusing on active-vs-passive detection differences, and spending too much time explaining why this instrument detects that much more high clouds here and that much less low clouds there. Those questions are valid, and require thorough discussions about the subtle interplay between instrumental sensitivities, the distribution of cloud properties on a global scale, and data analysis algorithmic choices, all of which require extensive studies of their own (e.g. Stubenrauch et al. 2012 which is 176 pages long). We were concerned that going down that path would detract the reader from the main novel results provided by CATS, i.e. the daily variability of the cloud vertical distribution. To do so we decided not to directly include retrievals based on ISCCP data. Instead, our goal was to verify that CATS retrievals capture the general qualitative feature of the daily cycle of cloud amounts, compared to the baseline dataset usually considered (ISCCP).

C. Stubenrauch, W. B. Rossow, and S. Kinne, 2012: Assessment of global cloud datasets from satellites: A project of the World Climate Research Programme Global Energy and Water Cycle Experiment (GEWEX) Radiation Panel. WCRP Rep. 23/2012, 176 pp.

17. L539-541: This could also due to the different day-night cloud detection sensitivities between lidar and ISCCP passive measurements.

This is a possible explanation that we now have included in the article. Thanks.

18. L574-579: You could try to use CALIOP 1064 only measurements to run the same detection to minimize the difference.

This could indeed diminish differences between CATS and CALIOP datasets that are related to the instrument's wavelength differences. Many other differences would remain, like laser pulse energy and repetition frequency (20Hz vs. 5kHz), beam width, telescope field of view, sampling rates, performance of optical elements, etc. Moreover, our focus here is on statistics over large regions and seasons, and the different altitude and orbital paths of both missions imply that comparisons will necessarily be statistical in nature — i.e. both datasets document different clouds anyway. Given this, it is unclear what understanding would be gained by going through the exercise suggested here.

The reviewer's suggestion will be useful though for future research aiming to clarify the reasons behind differences between CALIPSO and CATS cloud detections over case studies.

19. L585 "Cloud Fraction": either use CF or "cloud fraction".

Thanks for spotting this, we have corrected the error.

20. Section 5: It will good to have some discussion on the potential limitations here.

Section 5 now mentions the limitations of cloud fractions retrieved through spaceborne lidar measurements such as CATS and CALIOP, and highlights the problems that still need to be investigated.

Reviewer 3 comments and replies

“The diurnal cycle of cloud profiles over land and ocean between 51S and 51N, seen by the CATS spaceborne lidar from the International Space Station” by Vincent Noel et al.
This paper documents the diurnal cycle of the cloud vertical profiles over a large part of the globe, using CATS lidar, operating on the International Space Station. Cloud fractions from different locations, seasons, instruments have been compared, by taking the advantage of this unique dataset. The study is interesting and useful. But it would be better to relate the role of dynamic and thermodynamic processes to the differences of CF found from different conditions, which is not clearly presented. I recommend some modifications to improve the paper before publication.

We thank the Reviewer for his or her appreciation. Relating the cloud diurnal cycles documented in this paper to the other processes driving the daily evolution of the troposphere (temperature, water vapor) is the focus of a soon-to-be-submitted paper we are currently working on.

Major issues:

1. The second paragraph of Introduction needs more support references to help the readers to better understand the background. For example, ‘well documented by passive satellite imagery’, it would be better to add in relative works. The same suggestion for ‘b) cloud detections from ground-based active instruments’ part. There are a lot of works have been done with ground-based instruments on cloud property analysis, I would appreciate if you can give a few references here.

Our initial idea was that paragraph would sum up the findings of the articles referenced in the previous paragraph (“Those studies...”). However, the first paragraph only references studies of cloud diurnal cycles documented from space, whereas the findings in the second paragraph are general. Following this observation, we have rewritten the first two paragraphs of the introduction, trying to support our assertions with appropriate references.

This comment echoes minor issue #2 from reviewer 2.

2. The authors chose ARM SGP site for the comparison, is there any particular reason to compare two mid-latitude continental sites with CATS? Comparing with oceanic type of clouds would be interesting, if there are any possibilities. Since you actually didn’t really process the SGP dataset, I would suggest that you could keep this part as an additional material.

Following this comment, and major comment #3 from Reviewer 2, we have tried locating a well-documented, 24/24 dataset of cloud layers covering the period 2015-2017 based on measurements from a ground-based lidar operating in the Tropics, preferably close to the

ocean. We have contacted several observatories (e.g OPAR) but it appears lidar-based cloud layer products are often unvalidated and/or suffer from irregular or non-diurnal sampling.

Following the Reviewer's suggestion, we investigated ARM data [1] and found several datasets based on Tropics and/or oceanic measurements and promising cloud layer information. We found that:

- Datasets from Nauru Island and Darwin Australia did not overlap with CATS timeframe
- Datasets from Brazil and Ascension Island cover the CATS timeframe but only contained profiles of Attenuated Backscatter (without cloud detection) — doing the cloud detection ourselves would require external validation
- Only datasets from the ARM Eastern North Atlantic (ENA) atmospheric observatory [2] are close to our criterias above. This site provides cloud layers derived from ground-based lidar measurements made in an oceanic environment, unlike the SIRTA and ARM-SGP datasets considered in the initial article.

Since the ENA observatory is located at 39°N, it is at best sub-tropical. It is however the only oceanic ARM site we found that could provide a 24/24 robust cloud layers dataset covering the CATS time period.

Our initial exploration of the enaarsclkazrbnd1kolliasC1 dataset (based on a combination of lidar and radar data) showed unusual results during the 2017 summer (see figure below). We contacted ARM people, who explained the problem comes from unresolved issues with lidar cloud detections and suggested rebuilding the cloud layers based on the cloud mask source product and ignoring the lidar-only detections. This resolved the problem, but in effect turned it into a radar-based product.

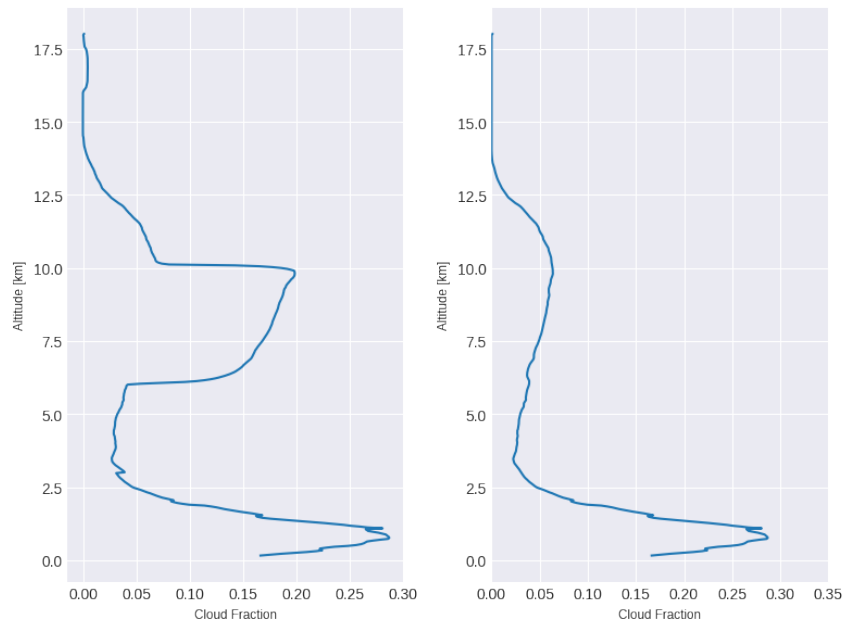


Figure 1 - Cloud fraction over ARM-ENA for 2017 JJA using both lidar and radar cloud detections (left) and radar-only cloud detections (right)

The paper now includes (Sect. 3.3) a direct comparison of the diurnal cycles of cloud fraction profiles as documented by CATS over the ENA site and from ground-based radar detections.

We have also obtained the ARM-SGP ground-based lidar+radar cloud detections in order to directly include them in the paper for comparison with CATS data. Exploration of the `sgparsclkazrbnd1kolliasC1` dataset showed artefacts similar to those from the ARM-ENA datasets (vertical steps in cloud fraction) when including lidar-only cloud detections. We thus had again to consider only radar detections, leading to results very similar to those presented in Zhao et al. (2016).

The fact that we uncovered issues with those ARM datasets, which are apparently among the most reliable, confirms how difficult it is to obtain faultless lidar-based cloud retrievals over long periods. Providing our own analysis of the data allowed us to only use cloud detections made during the CATS operation period, making time periods consistent across all ground-based comparisons.

The article now includes comparisons between CATS and:

- Lidar-based cloud retrievals from a midlatitude continental site (SIRTA), already described in e.g. Noel et Haeffelin (2006)
- Radar-based cloud retrievals from a midlatitude continental site (ARM-SGP), already described in e.g. Zhao et al. (2016)
- Radar-based cloud retrivals from a subtropical oceanic site (ARM-ENA).

We hope these improvements to our comparisons between CATS and ground-based datasets

better highlights the strengths and limitations of spaceborne and ground-based lidar cloud sampling.

[1] <https://www.arm.gov/data>

[2] <https://www.arm.gov/capabilities/observatories/ena>

3. You talked about the pronounced mid-level clouds over continent many times which has been well documented, could you give a more detailed explanation for that, and the role of dynamic and thermodynamic processes.

The mid-level clouds CATS detects over Africa, South America and Australia, in the North hemisphere in JJA and the South hemisphere in DJF, might very well be Altopcumulus clouds that Wang and Sassen (2012) document in the same locations, altitudes and times. This possibility is now discussed in the text.

Minor issues:

1. On Figure 1, is there any way to show the number of samples on the plots as well? In the text, the latitude range is 51S-51N, but on most of the plots, it's 55S-55N. It is better to keep it consistent.

Following this comment, the map in Figure 1 now shows the number of profiles sampled by CATS over the JJA 2015-2016-2017 period in 2°x2° grid cells. We thank the Reviewer for this suggestion that makes Figure 1 richer in information.

As noted by the Reviewer, the latitude ranges in figures and their legends were incorrect in the initial version of the manuscript we uploaded to ACPD in February. We fixed those in an updated version submitted in March (this version has “over land and ocean” in the title), which became the one available from the ACPD website during the open discussion [1]. We do not know why the reviewers were provided with the non-updated version and regret the confusion.

[1] <https://www.atmos-chem-phys-discuss.net/acp-2018-214/acp-2018-214.pdf>

2. The color bar need to be adjusted and extended to greater than 20%, add in unit, and keep the x axis and y axis consistent for the same figure group, specially figure 4.

Our attempts to increase the maximum to larger cloud fractions led to poor visibility for areas of weak cloud fractions, which are much more frequent and more frequently discussed in the text. Through experimentations, we found that limiting the color bar to a 20% maximum provided the best compromise between keeping variations of weak cloud fractions visible (e.g. at low altitudes) and not masking too many variations in large cloud fractions, for instance in high clouds in tropical summer conditions or low clouds over ARM-

ENA.

All cloud fraction colorbars should now include units (%). We have made sure all axes remain consistent within the same figure groups.

3. Figure 5, better to label A, B, C... on the subplot for each location.

We thank the reviewer for this useful suggestion that Figure 5 now implements.

4. Line 515: Using passive instruments to retrieve the cloud properties is different from active instruments, they don't have the same sensitivity for the thin clouds. It isn't a fair comparison here.

Our objective here is not to validate or depreciate either one of the detection approaches. All instruments have different sensitivities to different phenomenas. We do not think that confronting retrievals from passive instruments with retrievals from active instruments is unfair to the passive instruments — it shows how each instrument understands a scene, which we think helps the readers familiar with either one, or both, to understand what is actually going on. However, since the sentence in question did not bring any significant value to the manuscript, we have rewritten it to avoid any misunderstanding.

5. Another thing to note is that, besides cloud detection, retrieving a cloud top height from especially for thin clouds and in multi-layered situations.

We think some words are missing from the comment. We guess the Reviewer points out that cloud top heights retrieved from passive measurements can suffer from large uncertainties, especially in presence of thin clouds and multi-layered situations. We agree with his comment.

Reviewer 4 comments and replies

1. The paper discusses the diurnal changes in cloud fraction, but commonly CF is meant to represent the fraction of a grid box area or sensor field of view that is covered in cloud. Would it not be correct to give the results as cloud frequency instead, as that is what is actually being measured?

During the past years, interactions with co-authors and reviewers led to our adoption of the following naming scheme:

- "cloud cover" to name the fraction of a grid box area covered in cloud
- "cloud fraction profile" to name a vertical profile describing at each altitude level the fraction of shots containing clouds

Many articles use this distinction, for instance Reverdy et al. (2015), Chepfer et al. (2010) referenced in the main article. The following articles use the same naming scheme:

- Chepfer, H., Noel, V., Chiriaco, M., Wielicki, B., Winker, D., Loeb, N. and Wood, R.: The Potential of a Multidecade Spaceborne Lidar Record to Constrain Cloud Feedback, *J. Geophys. Res. Atmos.*, 123(10), 5433–5454, doi:10.1002/2017JD027742, 2018.
- Cesana, G., et al. (2016), Using in situ airborne measurements to evaluate three cloud phase products derived from CALIPSO, *J. Geophys. Res. Atmos.*, 121, 5788–5808, doi:10.1002/2015JD024334.
- Chepfer, H., V. Noel, D. Winker, and M. Chiriaco (2014), Where and when will we observe cloud changes due to climate warming?, *Geophys. Res. Lett.*, 41, 8387–8395, doi:10.1002/2014GL061792
- Reverdy, M., Noel, V., Chepfer, H., and Legras, B.: On the origin of subvisible cirrus clouds in the tropical upper troposphere, *Atmos. Chem. Phys.*, 12, 12081-12101, <https://doi.org/10.5194/acp-12-12081-2012>, 2012
- Chepfer H., S. Bony, D. Winker, M. Chiriaco, J-L. Dufresne, G. Sèze, 2008: Use of CALIPSO lidar observations to evaluate the cloudiness simulated by a climate model, *Geophys. Res. Lett.*, 35, L15704, doi:10.1029/2008GL034207.

We went through the paper to make sure that the paper always mentioned "cloud fraction profile", or specified an altitude range (e.g. "at low altitudes, cloud fractions are high..."). We hope this naming scheme is satisfactory.

2. Secondly, the figures' color bars max out at CF=20%, with values above 20% visible in many of the figures. It would be good to extend the color bar so that fewer figures saturate like this.

Our attempts to increase the maximum to larger cloud fractions led to poor visibility for areas of weak cloud fractions, which are much more frequent and more frequently discussed in the text (e.g. at low altitudes). Through experimentations, we found that limiting the color bar to a 20% maximum provided the best compromise between keeping

variations of weak cloud fractions visible and not masking too many variations in large cloud fractions, for instance in high clouds in tropical summer conditions or low clouds over ARM-ENA.

1 **The diurnal cycle of cloud profiles over land and ocean between 51°S and 51°N, seen by**
2 **the CATS spaceborne lidar from the International Space Station**

3

4 Vincent Noel ¹, H  l  ne Chepfer ², Marjolaine Chiriaco ³, John Yorks ⁴

5

6 1 - Laboratoire d'A  rologie, CNRS/UPS, Observatoire Midi-Pyr  n  es, 14 avenue Edouard
7 Belin, Toulouse, France

8 2 - LMD/IPSL, Sorbonne Universit  ,   cole polytechnique,   cole Normale Sup  rieure, PSL
9 Research University, CNRS, F-91120 Palaiseau, France

10 3 - LATMOS/IPSL, Univ. Versailles Saint-Quentin en Yvelines, France

11 4 - NASA GSFC, Greenbelt, Maryland, USA

12

13 Proposed for publication in:

14 Atmospheric Chemistry and Physics

15

16 19 June 2018

17

Deleted: 21 Mar 2018

19 **Abstract.**

20 We document, for the first time, how detailed vertical profiles of Cloud Fraction change
21 diurnally between 51°S and 51°N, by taking advantage of 15 months of measurements from
22 the Cloud and Aerosol Transport System (CATS) lidar on the non-sun-synchronous
23 International Space Station (ISS).

24 Over the Tropical ocean in summer, we find few high clouds during daytime. At night they
25 become frequent over a large altitude range (11-16km between 10PM and 4AM). Over the
26 summer tropical continents, but not over ocean, CATS observations reveal mid-level clouds
27 (4-8 km Above Sea Level or ASL) persisting all-day long, with a weak diurnal cycle (minimum
28 at noon). Over the Southern Ocean, diurnal cycles appear for the omnipresent low-level
29 clouds (minimum between noon and 3PM) and high-altitude clouds (minimum between
30 8AM and 2PM). Both cycles are time-shifted, with high-altitude clouds following the
31 changes in low-altitude clouds by several hours. Over all continents at all latitudes during
32 summer, the low-level clouds develop upwards and reach a maximum occurrence at about
33 2.5 km ASL in the early afternoon (around 2 pm).

34 Our work also shows that 1) the diurnal cycles of vertical profiles derived from CATS are
35 consistent with those from ground-based active sensors at local scale, 2) the cloud profiles
36 derived from CATS measurements at local times of 0130AM and 0130PM are consistent
37 with those observed from CALIPSO at similar times, 3) the diurnal cycles of low and high
38 cloud amounts derived from CATS are in general in phase with those derived from
39 geostationary imagery but less pronounced. Finally, the diurnal variability of cloud profiles
40 revealed by CATS strongly suggests that CALIPSO measurements at 0130AM and PM
41 document the daily extremes of the cloud fraction profiles over ocean and are more
42 representative of daily averages over land, except at altitudes above 10km where they
43 capture part of the diurnal variability. These findings are applicable to other instruments
44 with local overpass times similar to CALIPSO's, like all the other A-Train instruments and the
45 future Earth-CARE mission.

Deleted: e

Deleted: to document, for the first time, the diurnal cycle of detailed vertical profiles of Cloud Fraction between 51°S and 51°N

Deleted: After processing CATS lidar data, we analyzed the diurnal cycles of the cloud profiles over ocean and over continent in two different seasons. ¶

Deleted: the

Deleted: s geometric thickness increases

Deleted: significantly from 1km near 5PM to 5km near 10PM, resulting in a high clouds maximum at nighttime

Deleted: the presence of a

Deleted: layer

Deleted: ASL

Deleted:

Deleted: for the

Deleted: vertically

Deleted: show

Deleted: equally

67	Outline
68	1. Introduction
69	2. Data and methods
70	2.1 Data
71	a. Cloud detections from the CATS spaceborne Lidar
72	b. Cloud detections from ground-based active instruments
73	c. Cloud detections from passive and active spaceborne sensors
74	2.2 Methods
75	a. Building the diurnal cycle of Cloud Fraction profiles from lidar cloud detections
76	b. Building the diurnal cycle of Low and High Clouds Amounts from CATS data
77	3. Results
78	3.1 Diurnal cycle of Cloud Fraction profiles observed at Global scale
79	3.2 Diurnal cycle of Cloud Fraction profiles observed over mid-latitudes and Tropics
80	a. High clouds
81	b. Low clouds
82	c. Seasonal differences
83	3.3 Diurnal cycle of Cloud Fraction profiles above selected continental regions
84	a. Over South of Paris in Europe
85	b. Over the US Southern Great Plains ARM site
86	<u>c. Over the subtropical Eastern North Atlantic ARM site</u>
87	d. Over continents
88	4. Discussion
89	4.1 About the diurnal cycles of the Low and High Cloud Amounts
90	4.2 About the Cloud Fraction profiles observed at fixed local times by space lidars
91	5. Conclusions
92	

Formatted: Font: Not Bold, Not Italic

Formatted: Font: Not Bold, Not Italic

Deleted: c

94 **1. Introduction**

95 The diurnal cycle of clouds has been documented for decades by ground-based instruments
96 (e.g. Gray and Jacobson, 1977) and geostationary satellites (e.g. Rossow et al., 1989). Even
97 though climatologies give priority on how clouds change with seasons and geography, many
98 studies noted the strong diurnal cycle of boundary layer clouds. During the day, low clouds
99 form in the morning and expand, following the warming of the surface by incoming solar
100 radiation (Stubenrauch et al., 2006). Maximum low cloud amount is often reached in the
101 early afternoon. This sun-driven variation is maximum over continents, where it depends on
102 orography (Wilson and Barros, 2017; Shang et al., 2018), and in summer. It is more limited
103 over ocean and during winter (Rozendaal et al., 1995; Soden, 2000). When night falls,
104 condensation in the boundary layer can create stratiform clouds, which stabilize and expand
105 through nighttime radiative cooling at cloud top and reach maximal cover in the early
106 morning (Greenwald and Christopher, 1999; Eastman and Warren, 2014).
107 In the Tropics, the near-surface daily increase in water vapor triggered by solar warming
108 (Tian et al., 2004) is transmitted to higher altitudes through deep convection (Johnson et al.,
109 1999). This imposes a diurnal cycle to high clouds, which is delayed by several hours
110 compared to low clouds (Soden, 2000). Their maximum amount is reached in the evening
111 (Rossow and Schiffer, 1999; Stubenrauch et al., 2006). At midlatitudes, without deep
112 convection most of the troposphere is free from surface influence (Wang and Sassen, 2001),
113 and diurnal changes in the distribution of high-altitude clouds are limited. Changes are
114 rather driven by the local atmospheric circulation (e.g. Storm-tracks), leading to less
115 predictable patterns which are more location-dependent.
116 More recently, geostationary imagery documented the diurnal variations in the composition
117 of cloud cover above Central Africa (Philippon et al., 2016) and cloud top temperatures
118 (Taylor et al., 2017). In any case, the vertically-integrated nature of passive imagery means it
119 cannot resolve the vertical variability of clouds and its diurnal cycle, which is key to better
120 understand the atmospheric heating rate profile (L'Ecuyer et al., 2008). By comparison,
121 active remote sensing instruments, such as radars and lidars, document the cloud vertical
122 distribution with great accuracy and vertical resolutions finer than 500m. Long-running
123 datasets from active instruments operated from ground-based sites have led to useful time

Deleted: Cloud cover diurnal cycles have been documented from space by geostationary satellites as early as the late 1970's (e.g. Gray and Jacobson, 1977) and were summarized based on retrievals from the International Satellite Cloud Climatology Project (ISCCP; Cairns, 1994; Rossow and Schiffer, 1999). Soden (2000) and Tian et al. (2004) used those retrievals to confront the diurnal cycles of clouds, convective activity and water vapor in the upper troposphere, pointing to a clear land-sea contrast. More recently, Philippon et al. (2016) used MSG-SEVIRI data to describe the diurnal variations in the composition of cloud cover above Central Africa. Taylor et al. (2017) also used MSG-SEVIRI to describe when during the day the cloud top temperature is the coldest on average seasonally, over a half-hemisphere grid. Apart from geostationary imagery, few spaceborne instruments provide a sampling frequency well-suited to describe the diurnal variability of clouds. For instance, Wylie (2008) had to take advantage of the four observations per day provided by the NOAA series of polar orbiters to document a weakly-resolved clouds diurnal cycle from multispectral infrared data. ¶
Those studies found the most significant diurnal changes of clouds over continents in summer: low-level boundary layer clouds eand throughout the day, following the warming of the surface by incoming solar radiation, a process significantly affected by orography. In the Tropics, this near-surface activity is transmitted to higher altitudes through deep convection, driving a diurnal cycle in high-level clouds. The time needed for this process to occur delays the cycle of high clouds, whose maximas and minimas occur hours late compared to low-level clouds. At midlatitudes, without deep convection most of the troposphere is free from surface influence, and diurnal changes in the distribution of high-altitude clouds are rather driven by the local atmospheric circulation (e.g. Storm-tracks), leading to less predictable patterns. Over oceans, the largest low-level cloud covers happen in the morning, when the expansion generated by nighttime radiative cooling at cloud top stops. These patterns are supported by understood physical principles and are well documented by passive satellite imagery. But these observations do not provide information on the diurnal cycle of the detailed cloud profiles, which is key to better understand the atmospheric heating rate profile. ¶

- Deleted: A
- Deleted: er
- Deleted: resolutions than passive instruments, with
- Deleted: For decades, a
- Deleted: have been
- Deleted: , building extensive datasets from which

173 series and statistics about clouds (e.g. [Sassen and Benson, 2001](#); [Hogan et al., 2003](#); [Protat](#)
174 [et al., 2009](#); [Dong et al., 2010](#); [Hoareau et al., 2013](#); [Zhao et al., 2016](#)). From space, Liu and
175 Zipser (2008) were able to derive information on the clouds diurnal cycle from the
176 spaceborne Tropical Rainfall Measuring Mission radar, launched in 1997 (Kummerow et al.,
177 1998), but the instrument was not designed to detect clouds with accuracy. The CALIPSO
178 lidar (Cloud-Aerosol Lidar and Infrared Pathfinder Satellite Observations), since its launch
179 into orbit in 2006 (Winker et al., 2010), has provided transformative vertically-resolved data
180 on clouds (Stephens et al., 2017; Winker et al., 2017). Cloud detections from CALIPSO have,
181 among other things, helped pinpoint and improve significant cloud-related weaknesses in
182 climate models (e.g. Cesana and Chepfer, 2013; Konsta et al., 2016), helped improve
183 estimates of the surface radiation budget (Kato et al., 2011) and of the heating rate profile
184 (Haynes et al., 2013; Bouniol et al., 2016). Due to its sun-synchronous polar orbit, CALIPSO
185 samples the atmosphere at either 1:30AM or 1:30PM local time (LT), like the CloudSat radar
186 (Stephens and Kummerow, 2007) and all A-Train instruments (L'Ecuyer and Jiang, 2010).
187 Even though measurements at two times of day can offer insights into the day-night cloud
188 changes (Sèze et al., 2015; Gupta et al., 2018), they are insufficient to fully document the
189 diurnal evolution of cloud profiles. This observational blind spot explains why very little is
190 known so far about how the vertical distribution of clouds changes diurnally in most of the
191 globe, leading to inconsistencies amongst climate models (Yin and Porporato, 2017).

192 Here we take advantage of measurements from the Cloud Aerosol Transport System (CATS,
193 McGill et al., 2015) lidar on the International Space Station (ISS), to document the diurnal
194 evolution of the vertical distribution of clouds in regions of the globe. As the ISS orbits the
195 Earth many times a day between 51°S and 51°N, CATS measurements cannot track the
196 evolution of individual clouds over a given location and a given day. Instead, cloud
197 detections over a given location at variable times of day can be aggregated over seasons, to
198 create statistics that eventually document the seasonal average diurnal cycle of clouds over
199 that location. Thus far, the CATS dataset is the only one to contain active vertically-resolved
200 measurements made from satellite with variable local times of overpass.

201 We first describe how data were selected and processed to derive diurnal cycles of cloud
202 Cloud Fraction (CF) profiles and Cloud Amounts (CA) from CATS and all other instruments
203 included for comparison (Sect. 2). Then, using CATS retrievals we document, for the first

Deleted: can be derived

Deleted: Noel et al., 2006

Deleted: Enhanced c

Deleted: L'Ecuyer et al., 2008;

Deleted: However, d

Deleted: .

Deleted: T

Deleted: share the same overpass times

Deleted: limited to

Deleted: still

Moved down [1]: The CATS dataset is unique so far, as it contains active vertically-resolved measurements made by lidar from space with variable local times of overpass: the CATS lidar can document cloud profiles at different times along the day between 51°S and 51°N following the ISS orbit.

Moved (insertion) [1]

Deleted: T

Deleted: is

Deleted: unique so far, as it

Deleted: s

Deleted: by lidar

Deleted: space

Deleted: : the CATS lidar can document cloud profiles at different times along the day between 51°S and 51°N following the ISS orbit

228 time, the diurnal cycle of detailed Cloud Fraction profiles in large regions of the globe in two
229 seasons over ocean and land (Sect. 3.1 and 3.2). In Sect. 3.3 we describe CATS-derived
230 diurnal cycles of cloud profiles over selected sites and continents with two goals in mind: (i)
231 to compare them with independent ground-based observations to check the validity of the
232 CATS retrievals, and (ii) to document the diversity of the continental cloud profile diurnal
233 cycles over the globe. In Section 4 we discuss implications of our results: We compare the
234 diurnal cycle of the Low and High cloud covers derived from CATS with ones from
235 geostationary satellites (Sect. 4.1), and discuss the agreement between CATS Cloud Fraction
236 profiles derived at the times of CALIPSO overpass with actual CALIPSO retrievals (Sect.
237 4.2.a). Finally, we consider CATS profiles at overpass times from current and future sun-
238 synchronous spaceborne lidar missions (Sect. 4.2.b) to understand which part of the diurnal
239 cloud cycle is sampled by these instruments. We conclude in Sect. 5.

240 **2. Data and Methods**

241

242 **2.1 Data**

243

244 ***a) Cloud detections from the CATS spaceborne lidar***

245 In this study, our primary data consist of clouds detected during June-July-August (JJA) and
246 December-January-February (DJF) periods using data from the CATS lidar system (Yorks et
247 al., in preparation). CATS operated from the ISS between February 2015 to late October
248 2017. Although CATS was originally designed to operate at 3 wavelengths (355, 532 and
249 1064nm) with variable viewing geometries, beginning in March 2015 technical issues limited
250 operation to a single 1064nm wavelength and a single viewing mode. The CATS instrument
251 went on providing single-channel high-quality data (Yorks et al., 2016a) until a fault in the
252 on-board power and data system ended science operations on October 30, 2017.

253 Being located on the ISS means measurements from CATS are constrained to latitudes
254 below 51°, giving it access to ~78% of the Earth's surface (Figure 1, top). This prevents our
255 study from covering polar regions, but leads to densely distributed overpasses at latitudes
256 above 40°. CATS sampling is particularly good in populated midlatitude regions and above
257 the Southern Ocean.

258 CATS reports vertical profiles of Attenuated Total Backscatter (ATB) every 350m at 1064nm
259 with a 60m vertical resolution (Yorks et al., 2016a). In the mode 7.2 in which CATS operates
260 since February 2015, each profile is created by accumulating backscattered energy from 200
261 4kHz pulses, 20 times per second. The CATS vertical feature mask algorithms use these
262 calibrated ATB profiles, averaged to 5 and 60 km, to detect atmospheric layers, discriminate
263 clouds from aerosols, and determine cloud phase (Yorks et al., 2016b and in preparation).
264 The CATS layer-detection algorithms are based on a threshold-profile technique similar to
265 the one used for CALIOP (Vaughan et al., 2009) but, unlike for CALIOP, they rely primarily on
266 1064nm ATB (Yorks et al., 2016b). CATS cloud-aerosol discrimination algorithm uses a
267 probability density function technique that is based on the CALIPSO algorithm but relies on
268 horizontal persistence tests to differentiate low-level clouds and aerosol because
269 backscatter color ratio, used in the CALIOP algorithms (Liu et al., 2009), is not available in

Deleted: however

Deleted: . However, this

Deleted: :

273 Mode 7.2. For cloud phase, CATS uses layer-integrated 1064 nm depolarization ratio and
 274 mid-layer temperature thresholds based on Hu et al. (2009) and Yorks et al. (2011).
 275 Minimum horizontal average was 5km in nighttime and 60km in daytime, a choice that
 276 brings the same cloud detection sensitivity to both (Yorks et al., 2016a). This has two
 277 consequences: 1) optically thinnest clouds detected during nighttime at 60km horizontal
 278 averaging might be absent from daytime detections (these represent roughly ~5% of
 279 nighttime clouds) and 2) the horizontal extent and cloud amount of fragmented boundary
 280 layer clouds might be overestimated in both daytime and nighttime compared to single-shot
 281 detections (as in Chepfer et al., 2013; Cesana et al., 2016). Cloud top and base heights,
 282 phase, and other properties are reported in the CATS Level 2 Operational (L2O) products
 283 every 5 km along-track. Hereafter we used such cloud properties from CATS L2O data files
 284 v2.01 (Palm et al., 2016), including only layers with a feature type score above 5, to avoid
 285 including wrongly-classified optically thick aerosol layers near deserts.
 286 To document the diurnal cycle (Sect. 2.2.a), we used CATS cloud detections from JJA and DJF
 287 seasons between March 2015 and October 2017. CATS cloud data being still novel at the
 288 time of this writing, we document and discuss several of its characteristics in Appendices A
 289 and B, including sampling variability and the sensitivity of cloud detection in presence of
 290 solar pollution. This exploration of CATS data (and the upcoming comparisons with other
 291 instruments) made us confident that its sampling and cloud detections are robust enough to
 292 be used for scientific purposes.

Formatted: Font: Not Italic
 Formatted: Font: Not Italic

294 ***b) Cloud detections from ground-based active instruments***

295 Like with any lidar, the CATS laser beam gets fully attenuated when passing through clouds
 296 with optical depths larger than typically 3 (e.g., Chepfer et al., 2010). This can lead to the
 297 Cloud Fractions being underestimated in the lower troposphere. Meanwhile, horizontal
 298 averaging during daytime can lead to Cloud Fractions being overestimated at low altitudes.
 299 To estimate how much the CATS Cloud Fraction is biased at low altitudes, we compare CATS
 300 detections with independent observations collected from ground-based active instruments.
 301 Ground-based observation sites provide long-term records of atmospheric properties over
 302 periods that often cannot be reached by satellite instruments (Chiriaco et al., 2018).

Deleted: CATS cloud detections were derived from vertical profiles of ATtenuated Backscatter measured every 350m at 1064nm with a 60m vertical resolution. ATB profiles were calibrated, processed and averaged based on the procedures designed for CALIOP data to enable threshold-based cloud detection (Yorks et al., 2016b and in preparation). Unlike for CALIOP, the cloud detection algorithms for CATS rely primarily on 1064nm data. They create the CATS operational Level 2 (L2) products, which provide properties for detected clouds (including base and top) every 5km along-track. Hereafter we used such cloud properties from CATS L2O data files v2.01 (Palm et al., 2016), including only layers with a Feature_Type_Score above 5, to avoid including wrongly-classified optically thick aerosol layers near deserts. To document the diurnal cycle (Sect. 2.2.a), we used data obtained in both nighttime and daytime (sunlit) conditions between March 2015 and October 2017. ¶ CATS cloud data being still novel at the time of this writing, we document and discuss several of its characteristics in Appendices A and B, including sampling variability and the sensitivity of cloud detection in presence of solar pollution. This exploration of CATS data (and the upcoming comparisons with other instruments) made us confident that its sampling and cloud detections are robust enough to be used for scientific purposes. ¶

Deleted: c
 Deleted: f
 Deleted: c
 Deleted: f
 Deleted: in revision

333 Nowadays such sites are often well equipped with active remote sensing instruments. Data
334 acquisition, calibration and processing are often homogenized in the framework of specific
335 observation networks (e.g. EARLINET, the European Aerosol Research Lidar Network,
336 Pappalardo et al., 2014). Descriptions of the clouds diurnal cycle based on active ground-
337 based measurements are however scarce. In this study, we compare CATS cloud cycles with
338 those derived from active measurements at three ground-based sites, two continental and
339 one oceanic;

- The Site Instrumenté de Recherche par Télédétection Atmosphérique (SIRTA, Haeffelin et al., 2005) is continental, located 20km South-West of Paris at 48.7°N, 2.2°E. From SIRTA we used cloud detections from the Lidar Nuages et Aérosols (LNA, Elouragini and Flamant, 1996), which were curated, packaged and made available in the framework of the SIRTA-reOBS project (Chiriaco et al., 2014, 2018). The LNA requires human supervision and does not operate under precipitation, leading to irregular sampling and almost no nighttime measurements. Thanks to its long operation time, its cloud dataset covers almost 15 years and was used in many studies (e.g. Noel and Haeffelin, 2007; Naud et al., 2010; Dupont et al., 2010). Cloud layers were detected in LNA profiles of attenuated backscatter following a threshold-based approach similar to CATS and CALIPSO.

- The Atmospheric Radiation Measurement (ARM) Southern Great Plains (SGP) site is continental too, at 97°W, 36°N. From ARM-SGP we used the sgparsclkazr1kolliasC1 cloud dataset (DOI: 10.5439/1393437), which contains vertical cloud detection profiles for every second every day based on measurements from the 35GHz Ka ARM Zenith Radar. This instrument has been operating since 2011 (Kollias et al., 2014). Based on these profiles we reconstructed hourly averages of Cloud Fraction profiles over seasons during the CATS operation period. Our results closely match those Zhao et al. (2017) derived from the same instrument, and those Dupont (2011) derived from the ARM-SGP Raman lidar;

- The ARM Eastern North Atlantic (ENA) site is oceanic, located on Graciosa Island in the Azores archipelago (28.03°W, 39.1°N). From ARM-ENA we used cloud detections from the enarsclkazr1kolliasC1 dataset derived from a 35GHz radar similar to the one found at SGP, which we processed in a similar way;

Deleted: two

Deleted: in Europe and the United States

Deleted: .

Formatted: Font: 12 pt

Formatted: List Paragraph, Bulleted + Level: 1 + Aligned at: 0,63 cm + Indent at: 1,27 cm

Deleted: first ground-based site is the

Deleted: ,

Formatted: Font: 12 pt

Deleted: observations

Deleted: . Cloud detections from the LNA were homogenized

Deleted: re

Deleted: ; Chiriaco et al.,

Deleted: in revision

Deleted: I

Formatted: Font: 12 pt

Formatted: Font: 12 pt

Deleted: however means

Formatted: Font: 12 pt

Deleted: second site we consider is the

Formatted: Font: 12 pt

Deleted: this ground-based site

Formatted: Font: 12 pt

Deleted: consider

Deleted: retrievals

Deleted: from the Millimeter Wavelength Cloud Radar (MMCR) and from the Raman Lidar (RL). The MMCR has been routinely

Deleted: ed to detect and identify clouds and precipitations

Deleted: 1996

Deleted: Moran et al., 1998

Deleted:), while RL cloud detections are available since [1]

Deleted: In the framework of the present study we did [1]

Formatted: Font: 12 pt

Moved (insertion) [2]

Deleted: Fig. 3a, top left

Deleted: i

Deleted: n Zhao et al., 2017

Formatted: Font: 12 pt

Formatted: Font: 12 pt

Formatted: Font: 12 pt

Formatted: Font: 12 pt

Formatted: Font: Bold

402

403 **c) Cloud detections from passive and active spaceborne sensors**

404 In addition to the ~~datasets from~~ CATS, LNA and ~~two ground-based radars~~, in the
405 upcoming sections we use cloud retrievals from two spaceborne datasets to put CATS cloud
406 retrievals into a referenced context. First, we consider the baseline reference for the
407 description of the clouds diurnal cycle from space: the analysis of data from the ISCCP done
408 by Rossow and Schiffer (1999), hereafter RS99. Their results are based on aggregated and
409 homogenized infrared and visible radiances from imaging radiometers on the international
410 constellation of weather satellites. They are widely considered as the reference for
411 describing the diurnal cycle of the cloud cover at large scales from space measurements. ~~We~~
412 did not reprocess any ISCCP data for the present study, instead we rely on the description of
413 the diurnal cycle of low and high clouds RS99 documented in their Fig. 11 based on ISCCP, to
414 which we confront CATS retrievals in Sect. 4.1.

415 Finally, we also confront CATS cloud detections with retrievals based on measurements
416 from the CALIOP lidar, routinely made since 2006 from the sun-synchronous CALIPSO
417 platform at 13:30 and 01:30 LT in Sect. 4.2. To enable comparison with CATS retrievals, we
418 used cloud layers retrieved from CALIPSO measurements during the period of CATS
419 operation (March 2015 to October 2017), and documented at ~~a~~ 5km horizontal resolution in
420 CALIPSO Level 2 V4.10 Cloud Layer Products (Vaughan et al., 2009). We processed both
421 CATS and CALIPSO data alike as described in Sect. 2.2.a.

422

423 **2.2. Methods**

424

425 **a) Building the diurnal cycle of Cloud Fraction profiles from lidar cloud detections,**
426 Analyzing CATS lidar echoes lets one identify at which altitude a cloud is present above a
427 particular location on Earth at a given moment. By aggregating such information over a long
428 period, vertical profiles of Cloud Fraction can be derived. A CF(z) profile documents at which
429 frequency clouds were observed at the altitude z over a particular location. Cloud Fractions
430 are conceptually equivalent to the Cloud Amounts derived from passive measurements

Deleted: MMCR

Deleted: datasets

Deleted: Like with SGP data, w

Formatted: Left, Indent: First line: 0 cm

Deleted: ,

Deleted: .¶

Deleted: ¶

Formatted: Numbered + Level: 1 + Numbering Style: a, b, c, ... + Start at: 1 + Alignment: Left + Aligned at: 0,63 cm + Indent at: 1,27 cm

Deleted: (CF)

438 (next section), but vertically resolved with a 60 meters resolution.

439 From CATS level 2 data files, we extract profile-based cloud detections and use the
440 measurement UTC time and coordinates to deduce their local time of observation. Using the
441 resulting list of cloud layer altitudes, coordinates and local times of detection, we count the
442 number n of cloud detected within half-hour bins of local time, $2^\circ \times 2^\circ$ lat-lon boxes and
443 200m altitude bins. We also count the number of valid data points n_0 within those bins.

444 Eventually, we derive the Cloud Fraction $CF = \frac{n}{n_0}$, either in individual local time/lat-
445 lon/altitude bin or by aggregating n and n_0 over a selection of bins. Thus, we recreate a
446 statistically accurate representation of the diurnal cycle of Cloud Fractions profiles, over any
447 location between 51°S and 51°N, through the aggregation over long periods of cloud
448 detections made over that location on different days and local times.

449 CATS reports cloud layers as opaque when no echo from the surface is found in the profile
450 below a detected cloud, following the same methodology as in Guzman et al., 2017. Below
451 an opaque cloud layer, there is no laser signal left to propagate, and clouds potentially
452 present at lower altitudes will not be sampled by the lidar. To account for this effect, we
453 consider the portions of profiles below an opaque layer unsampled, and they do not count
454 in the number of valid data points n_0 . This approach limits the influence of laser attenuation
455 on cloud detections but cannot totally cancel it. For very low clouds (top below 2km), we
456 make an exception to this rule and consider the lower part of the profile cloudy, as we
457 found this creates the best agreement with ground-based observations.

458 To enable comparisons with CATS CF profiles (Sect. 3.3 and 4.2), we followed a similar
459 approach to build CF profiles using cloud detections from SIRTa-reOBS and ARM datasets
460 (Sect. 2.1), and from CALIPSO Level 2 products (Sect. 2.1.c). In both cases, we counted the
461 number of cloud detections and valid (non-attenuated) measurements in hourly local time
462 bins and 200m altitude bins. For CALIPSO, only 01:30AM and PM time bins were filled.

463

464 ***b) Building the diurnal cycle of Low and High Cloud Amounts from CATS data***

465 As ISCCP data are based on radiances, clouds therein are characterized according to
466 their retrieved top pressure P as low ($P > 680\text{hPa}$), middle ($440 < P < 680\text{hPa}$) or high
467 ($P < 440\text{hPa}$). To enable a direct ISCCP-CATS comparison, we derived Cloud Amounts (CA)

Deleted: ,

Deleted:

Deleted: .b

Deleted: ¶

472 from CATS data for low and high clouds as defined by altitude: low clouds have their top
473 below 4km ASL, high clouds have their base above 7km, and mid-level clouds are in
474 between. Using the list of cloud layer altitudes, coordinates and local times of detection
475 derived from CATS detections (Sect. 2.2.a), we count the number of occurrences n' of at
476 least part of one cloud layer in half-hour bins of local time, $2^\circ \times 2^\circ$ lat-lon boxes and the three
477 altitude ranges (0-4km, 4-7km and higher than 7km ASL). We also count the number of
478 occurrences n'_0 that could possibly be reported given the measurements sampled by CATS
479 within each bin, taking into account the existence of opaque layers. Eventually, we derive
480 the Cloud Amount $CA = \frac{n'}{n'_0}$ for low, mid and high-altitude clouds layers, either in individual
481 local time/lat-lon bin or by aggregating n' and n'_0 over a selection of bins. Like RS99, we
482 separated CATS cloud detections over land and ocean, based on the International
483 Geosphere-Biosphere Programme surface flag present in CATS L2 products on a profile basis
484 (Palm et al., 2016).

Deleted: base

Deleted: tops

487 **3. Results**

488 **3.1. Diurnal Cloud Fraction profiles observed at Global scale**

489
490 Figure 1 shows the global diurnal cycle revealed by CATS during JJA from March 2015 to
491 October 2017 over Ocean and Land (bottom left and right). Low and high clouds are clearly
492 separated, with a band of minimum cloudiness in-between (near 4km ASL). Above both
493 surfaces, CATS data show an increase of high clouds during nighttime. Sassen et al. (2009)
494 explain this increase by the infrared radiative cooling of the upper troposphere. The vertical
495 spread of high clouds is most narrow near noon, at which point their apparent base is the
496 highest. These findings are consistent with CALIPSO retrievals (Sassen et al., 2009; Gupta et
497 al., 2018). The vertical evolution in the fraction of sampled atmosphere due to attenuation
498 by atmospheric components, for these diurnal cycles and all that follow, is documented in
499 Appendix C.

500 Significant differences exist between the cloud profiles diurnal cycle above land and ocean.
501 Clouds generally extend higher over land during nighttime: high clouds are vertically most
502 frequent near 10km over ocean, while they extend up to 14km above continents until 5AM.
503 Over ocean, high clouds appear to rise late in the afternoon (3-6PM) and fall soon thereafter
504 as the sun sets. Land-ocean differences are most striking at low altitudes: over Ocean low
505 clouds are present almost all day long between 0 and 2km ASL, their CF decreasing from a
506 20% maximum near 4AM to ~10% between 11AM and 5PM. Over land, low clouds are most
507 significant during daytime: they appear near 2km ASL at 10AM and extends upwards to
508 reach 4km ASL near 4PM. The associated CF remains low, at most 8%. These planetary
509 boundary layer (PBL) clouds are most certainly associated with turbulence and convection
510 activity occurring near the surface. They disappear after 4PM without connecting to the
511 higher layers. The clear-sky band (CF < 2%) near the surface is largest at night (almost 2km)
512 and thinnest in the late morning.

513 An aside on cloud detection: over the ocean, CATS detects more low and high clouds during
514 nighttime. This means that the increase in high clouds does not prevent the lidar
515 measurements to represent faithfully at least part of the nocturnal increase in low clouds.

Deleted: f

Deleted: shows the global diurnal cycle revealed by CATS data over Ocean and Land during JJA from March 2015 to October 2017

Deleted: Above Sea Level or

Deleted: large amounts of

Deleted:

Deleted: that get thinner near

Deleted:

Deleted: as their base rise

Deleted:

Deleted: night falls

Deleted: only

Deleted: thickest

Deleted: both

Deleted: more frequently

532 During daytime, the decrease in detection sensitivity due to solar pollution could
533 underestimate the retrieved frequency of clouds (low or high). However, CALIPSO cloud
534 detections also reveal a nighttime increase in high clouds, which Sassen et al. (2009) and
535 Gupta et al. (2018) found much too large to be attributed to detection bias from solar noise.
536 Since CATS daytime cloud detection abilities at 1064nm are at least as good as CALIOP's at
537 532nm (Yorks et al., 2016), it follows that CATS cloud retrievals should provide a reliable
538 qualitative assessment of their diurnal cycle, as comparisons with ground-based
539 measurements will later show (Sect. 3.3). How much solar noise leads to an underestimate
540 of high clouds in CALIOP and CATS datasets still needs to be quantified.
541 While these seasonal mean results are informative, they mix together unrelated cloud
542 populations from hemispheres with opposite seasons driven by different circulation
543 regimes. We thus describe the daily cycles of clouds in zonal bands in the next section.

Deleted: suggests that the high clouds are optically thin enough for letting CATS document the increase of lower clouds. If the reverse was true, more high clouds would be systematically linked to fewer low clouds, which is not what we observe. The frequency of high-level clouds observed in daytime could however be affected by

Deleted: cloud

Deleted: affecting the signal to noise ratio

Deleted:

Deleted: While CATS is seeing the diurnal cycle of high and low clouds, the magnitude of the daytime cloud fractions could then be biased slightly low due to solar pollution and, at low altitudes, cloud-aerosol discrimination issues.

Formatted: Left, Space After: 6 pt, Line spacing: 1,5 lines, No widow/orphan control, Don't adjust space between Latin and Asian text, Don't adjust space between Asian text and numbers, Tab stops: 0,63 cm, Left + 1,27 cm, Left + 1,9 cm, Left + 2,54 cm, Left + 3,17 cm, Left + 3,81 cm, Left + 5,08 cm, Left + 6,35 cm, Left + 7,62 cm, Left

Deleted: ¶

558 **3.2. Diurnal Cloud Fraction profiles observed over mid-latitudes and Tropics**

559 In this section, we consider cloud populations over four latitude bands: midlatitude (30°-
560 51°) and Tropics (0-30°), in the North Hemisphere (NH) and South Hemisphere (SH), over
561 land and ocean. We first examine the differences between the diurnal cycles affecting the
562 cloud vertical profiles over ocean and land in JJA (Sect. 3.2.a and 3.2.b, Fig. 2), then we
563 discuss how these cycles are affected by the season by considering DJF results (Sect. 3.2.c,
564 Fig. 3).

565

566 *a) High clouds*

567 As expected, Fig. 2 shows that high clouds are located at higher altitude in the tropics (12-
568 16km ASL) than in midlatitude (8-12km), following the variation of the troposphere depth
569 with latitude. Also as expected, the occurrence of high clouds is largest (CF > 20%) in deep
570 convection along the Inter-Tropical Convergence Zone (ITCZ), located between 0° and 30°N
571 in JJA, and minimum (CF < 8%) in the subsidence branch of the Hadley cell (0°-30°S in JJA). In
572 mid-latitudes, high clouds (7-9km ASL) are far more frequent (CF ~ 20%) over the Southern
573 Ocean (30°S-51°S) than over the northern ocean (30-51°N).

574 The CF of oceanic high clouds follows a strong diurnal cycle, with a maximum at nighttime
575 and a minimum at noon, in mid-latitudes and tropics (even in subsidence region). This cycle
576 is more pronounced where the high clouds are more numerous: along the ITCZ (0-30°N) and
577 in the Southern Ocean (30-51°S). In addition to the variation in the high cloud occurrence,
578 the vertical distribution of these clouds also follows a marked diurnal cycle along the ITCZ:
579 detections spread vertically over more than 4km near midnight, but over less than 1km at
580 noon. This spreading out occurs between 5PM and 10PM, and disappears much faster
581 during the morning. A wider spread of detection altitudes can either indicate the presence
582 of geometrically thicker clouds, or a wider distribution of optically thick clouds tops only
583 partially sampled by CATS. By comparison, over the Southern Ocean, high cloud detections
584 occur over the same altitude range throughout the day.

585 Overall, high clouds behave very similarly above land (Fig. 2, right column) and ocean (Fig. 2,
586 left column) at all latitudes, except between 30-51°S where the continental surface is too
587 small to conclude.

Deleted: Cloud fraction profile

Deleted: s

Deleted:

Deleted: O

Deleted: CF exhibits

Deleted: a marked

Deleted: a pronounced

Deleted: midday

Deleted: all latitude ranges (

Deleted: and mid latitudes

Deleted:)

Deleted: Even if t

Deleted: strong diurnal

Deleted: occurs at all latitudes (even in subsidence region), it

Deleted: extent

Deleted: shows

Deleted: as well

Deleted: thickening

Deleted: takes a few hours

Deleted: (

Deleted: -

Deleted:)

Deleted: while

Deleted: thinning is much sharper

Deleted: the thickness of

Deleted: s

Deleted: remains quite stable

Deleted: land

616

617 *b) Low clouds*

618 Over ocean in JJA (Fig. 2), the occurrence of low clouds (0-3km ASL) changes significantly
619 with latitude: The Southern Ocean region (30-51°S) is by far the cloudiest, the mid-latitude
620 north (30-51°N) and the subsidence tropics (0-30°S) are moderately cloudy, and even less
621 low clouds are observed along the ITCZ (0-30°N). The oceanic low clouds show only small
622 variations along the day. A weak diurnal cycle occurs at all latitudes except along the ITCZ
623 (possibly because low clouds there are in part masked by higher clouds affected by an out-
624 of-phase diurnal cycle). Low-level clouds are more numerous in nighttime (CF near 20%)
625 compared to daytime (CF~12%) in subsidence tropics (0-30°S) and mid-latitude north (30-
626 51°N). The southern oceanic low clouds exhibit a very faint diurnal cycle: their CF gets over
627 20% nearly all day long, with a very small decrease near 2PM.

Deleted: there the

628 In contrast to high clouds, the differences between land and ocean are striking for the low
629 and mid-level clouds. Both the occurrences and the diurnal cycles of clouds over land differ
630 significantly from their oceanic counterparts. The low clouds are very few over land (CF~4%)
631 compared to over ocean (>16%), all day long. Moreover, the continental low cloud diurnal
632 cycle exhibits a maximum in the early afternoon (around 2PM) that does not show up over
633 ocean: a maximum CF appears around 2.5 km of altitude in the upper edge (or just above
634 the top) of the atmospheric boundary layer; it is linked to convective activity between 10AM
635 and 5PM.

636 Another noticeable difference between land and ocean is the presence of well-defined mid-
637 level cloud population over NH tropical land (0-30°N, 2nd row on the right in Fig. 2) in the
638 free troposphere between 5 and 7 km ASL. These mid-level clouds show a diurnal cycle
639 opposite to PBL clouds and similar to the high clouds in that its minimum occurs at midday
640 and its maximum at night, although the magnitude of this cycle is much more limited. This
641 altitude range would be consistent with cumulus congestus (Johnson et al., 1999). Those,
642 however, are present above both land and ocean (Masugana et al. 2005) and CATS finds little
643 clouds at these altitudes over ocean. Rather, the clouds altitudes and location, over land in
644 the summer hemisphere, are consistent with Altocumulus clouds as described by Sassen and
645 Wang (2012) using CALIPSO and CloudSat measurements. Bourgeois et al. (2017) discussed
646 the diurnal cycle of similar clouds observed over West Africa: they found these clouds reach

648 maximum occurrence early in the morning, which is consistent with our results.

649

650 *c) Seasonal differences*

651 Figure 3 presents diurnal cycles of Cloud Fraction profiles over the same latitude bands as
652 Fig. 2 but based on data collected during the boreal winter (DJF). As seasons switch
653 hemispheres, we anticipate cloud populations to undergo symmetric changes across
654 hemispheres, in agreement with large-scale dynamic processes driving their spatial
655 distribution on seasonal time scales. This is verified for high clouds (Fig. 2 vs. Fig. 3): in the
656 Tropics the ITCZ moves to South and with it the large CF at high altitudes, in midlatitudes the
657 high clouds are more frequent during the winter season, due to more frequent low-pressure
658 conditions.

659 Interestingly, the mid-altitude clouds visible near 6km ASL in the NH Tropics over land (Fig. 2,
660 2nd row on the right) also move to the SH Tropics in DJF (Fig. 3, 3rd row on the right). This
661 confirms the year-long persistence of midlevel clouds over continental tropical regions found
662 by Bourgeois et al. (2017).

663 The seasonal changes in low clouds are less symmetric than in higher clouds, as they are
664 more closely related to surface conditions. Over ocean, in DJF the amount of low clouds
665 increases dramatically in NH midlatitudes compared to JJA (Fig. 2 and 3, top left), but does
666 not change noticeably in the SH midlatitudes: the diurnal cycle that sees a slight decrease in
667 the huge population of low clouds over the Southern Ocean is present in both seasons (Fig.
668 2 and 3, bottom left). Over land, in the Tropics, low clouds appear similar in frequency and

669 behavior in both DJF and JJA: PBL clouds extend vertically between ~7AM to 5PM (Fig. 2 and
670 3, rows 2 and 3 of right column). The NH midlatitudes show the strongest seasonal change in
671 low clouds, as they become present all day long: the diurnal cycle associated with PBL
672 development in JJA disappears in DJF (Fig. 2 and 3, top right). SH midlatitude retrievals over
673 land are noisy in DJF and JJA, but the DJF data (Fig. 3, bottom right) suggests that low clouds
674 there extend vertically a lot more than in JJA, up to 4km ASL.

Deleted: c

Deleted: f

Deleted: u

Deleted: as

679 **3.3. Diurnal cycle of cloud profiles above selected continental regions**

680

681 In this section, our first goal is to compare the diurnal cycle of the Cloud Fraction profiles
682 from CATS against independent observations collected by active instruments from ground-
683 based sites (Sect. 3.3.a and 3.3.b). In particular, we want to understand if the behaviors
684 found so far (Fig. 1-3) are valid for low clouds despite the attenuation of the space laser
685 signal (Sect. 2.2.a). Our second goal is to compare, for the first time, the diurnal cycle of the
686 Cloud Fraction profiles over different continental regions all over the globe as observed with
687 a single instrument (Sect. 3.3.c).

Deleted: c

Deleted: f

Deleted: results

Deleted: shown

Deleted: c

Deleted: f

688 It is important to note that since detection sensitivity, penetration depths and algorithmic
689 choices (e.g. averaging times and distances) change significantly from one instrument to the
690 next, we do not expect the various datasets to agree on absolute values of Cloud Fraction
691 profiles or Cloud Amounts. Rather, our interest is in whether different instruments agree on
692 the behavior of the diurnal evolution of clouds when they document the same location.
693 Thus the following comparison focus on the main features of the daily cycles and not on
694 absolute values.

695

696 **a) Over South of Paris in Europe**

697 Figure 4 shows the diurnal evolution of CF profiles seen by the ground-based LNA lidar (top
698 left) operated on the SIRTA site south of Paris (Sect. 2.1.b) and seen by CATS in a 10°x10°
699 box centered on SIRTA, keeping only profiles sampled over land (top right). Both datasets
700 report a well-defined high-altitude layer, with a clear-cut cloud top near 12 km ASL that
701 rises up a few hundred meters in the morning until 10AM and slowly falls during the
702 afternoon by at most 1 km. In both figures, the bottom of this layer is not sharply defined:
703 the CF decreases almost linearly from 11-12km ASL to near-zero at 4km ASL. Both
704 instruments also report a low-level cloud layer that initiates in the morning and extends
705 upwards from ~1km ASL at 5AM to ~4km ASL near 8PM.

Deleted: Fig. 4a

Deleted: space lidar

Deleted: the same site

Deleted: Fig. 4b

Deleted: from 20% near

Deleted: the space lidar

Deleted: a late-afternoon resurgence of high-altitude clouds (starting near 5PM)

Deleted: absent from the ground-based lidar record

Deleted: The space lidar

Deleted: also

Deleted: a much lower frequency of

706 Regarding differences, CATS sees more high-altitude clouds. In the late afternoon (starting
707 near 5PM), in particular, the ground-based lidar instead sees much less high clouds; that
708 instrument, however, suffers from poor sampling at this late hour. CATS reports less

727 boundary layer clouds, particularly in the late afternoon, when the ground-based lidar
 728 reports low-level CF above 20% (again, a time of poor sampling). The large number of high-
 729 altitude clouds observed by CATS at that time could impair its ability to detect lower clouds,
 730 while at the same time the many low clouds observed by the ground lidar can impair its
 731 ability to detect high clouds. The absence of precipitating clouds from the LNA dataset could
 732 also explain this difference.

- Deleted: : less than 10% throughout the day. This difference gets
- Deleted: large
- Deleted: the
- Deleted: rising
- Deleted: quantity
- Deleted: large quantity of

733
 734 **b) Over the US Southern Great Plains ARM site**

735 Figure 4 shows the diurnal evolution of CF profiles seen by the SGP-based radar (2nd row,
 736 left) and CATS (right) in a 10°x10° lat-lon box centered on the SGP site (Sect. 2.2.b), keeping
 737 only profiles sampled over land. During nighttime, both datasets report frequent high-level
 738 clouds near 12km ASL with large CF between 16:00 and 03:00 LT. At night, high clouds are
 739 also more distributed vertically, between 9 and 14km ASL. CATS and SGP datasets agree that
 740 the importance of high-level clouds strongly drops during daytime (7AM-5PM), with a
 741 minimum CF at midday. During daytime, the vertical distribution of high-level clouds is more
 742 narrow, from 11 to 12km ASL at its thinnest point (near 10AM). This rather strong cycle of
 743 high-level clouds can be explained by possible influence from Tropical dynamics at the 36°N
 744 latitude of the SGP site. There are slightly more midlevel clouds (4-8km ASL) at night, with
 745 increasing CF between midnight and 7AM. PBL clouds form near the surface at 9AM, rise
 746 and thicken almost up to 4km ASL near 4PM.

Deleted: As expected, the spaceborne CATS lidar sees more high-level clouds and less low-level clouds than the ground-based LNA lidar. This sampling bias affects all ground-space lidar comparisons (e.g. Dupont et al., 2010). Even so, the diurnal cycle of the cloud altitudes are roughly consistent from space and ground lidars. This comparison suggests the main limitation of CATS is the capability to document the increase in low cloud occurrence in the late afternoon. ¶

- Deleted: c
- Deleted: based on
- Deleted: measurements
- Deleted: the ARM
- Deleted: H
- Deleted: Above Sea Level (
- Deleted:)
- Deleted: are frequent during nighttime,
- Deleted: (above 20%)
- Deleted: The
- Deleted: layers
- Deleted: get thick and extend
- Deleted: T
- Deleted: dropping below 10%
- Deleted: The associated
- Deleted: cloud
- Deleted: layer gets much
- Deleted: thinner
- Deleted: limiting its extent between
- Deleted: and
- Deleted: in the early morning
- Deleted: increasing to ~10%
- Moved (insertion) [3]

747 There are of course differences. The SGP radar detects PBL and midlevel clouds twice more
 748 frequently than CATS, even though few high clouds are present. CATS also misses low-level
 749 clouds observed by the SGP radar between 6PM and 6AM, probable stratiform clouds that
 750 could either be too optically thin for CATS or miscategorized by its cloud detection
 751 algorithm.

Formatted: Indent: First line: 0 cm

Deleted: Midlevel clouds are almost non-existent the rest of the day. PBL clouds form near the surface at 9AM, rise and thicken almost up to 4km ASL near 4PM.

Moved up [3]: PBL clouds form near the surface at 9AM, rise and thicken almost up to 4km ASL near 4PM.

752
 753 **c) Over the subtropical Eastern North Atlantic ARM site**

754 Figure 4 shows the diurnal evolution of CF profiles seen by the ENA-based radar (bottom
 755 row, left) and CATS (right) in a 10°x10° lat-lon box centered on the ENA site (Sect. 2.2.b). The
 756 vertical distribution of clouds appears very different over this oceanic site. Both CATS and

Deleted: ¶

Formatted: Font: Bold, Italic

800 the ENA radar agree on the day-long persistence of low-level clouds below 2km ASL, and on
 801 their slight drop in Cloud Fraction and vertical spread between noon and 6PM. This is
 802 consistent with persistent stratiform clouds that are maximum at night. CATS sees more
 803 high clouds (8-12km ASL) than the ENA radar (4-12km ASL). CATS also reports a Cloud
 804 Fraction minimum between 0300-0500LT that is not present in ground-based dataset.
 805 These three comparisons between CATS and ground-based measurements suggest that, in
 806 general, the spaceborne lidar sees more high-level clouds and the ground-based instrument
 807 more low-level clouds. This sampling bias affects all space lidar comparisons with ground
 808 instruments (e.g. Dupont et al., 2010). Even so, we find similar behavior in the diurnal cycles
 809 reported by CATS and ground instruments over the same locations. Dataset discrepancies
 810 appear acceptable given the much smaller size of the CATS dataset (infrequent overpasses
 811 over 3 seasons, compared to daily local measurements) and the instrumental and
 812 algorithmic variations already mentioned. It is reassuring to find that CATS results retain the
 813 major features of the clouds profile daily cycle, most notably, an acceptable representation
 814 of the daytime low-level boundary layer clouds at all three sites, despite the presence of
 815 high-level clouds.
 816 In this section, we have seen that retrievals from ground-based instruments suggest CATS
 817 measurements reliably document the clouds diurnal cycle. Due to the distribution of
 818 ground-based sites, however, this approach is limited to mostly midlatitudes from the
 819 Northern Hemisphere. Next, we compare CATS detections with global spaceborne
 820 retrievals.

822 **d) Diurnal cycles of the cloud profiles over continents**

823 Continents are diverse in ground type, orography, latitude, exposition to large-scale
 824 atmospheric circulation, and transport of air masses from the local environment. These
 825 factors influence the atmosphere above the continent, leading to possible variations in the
 826 cloud diurnal cycle profiles. Ground-based observations let us document these different
 827 cycles, but differences between instruments and operations in the different ground sites
 828 make comparing diurnal cycle observed from ground at different locations difficult. Thanks
 829 to CATS data, for the first time we compare here the cloud diurnal cycle profiles observed
 830 over different continents by a single instrument and with a relatively large space sampling,

Moved up [2]: Fig. 3a, top left in Zhao et al., 2017

Deleted: Most of these features derived from CATS observations are consistent with those derived from summer observations by the ground-based MMCR (Fig. 3a, top left in Zhao et al., 2017) and RL (Fig. 3, bottom right in Dupont et al., 2011 -- mind the x-axis in UTC, which brings the local noon at 18UTC). For instance, Both CATS and the ground-based datasets report a rather strong diurnal cycle of high clouds, which can be explained by possible influence from Tropical dynamics at the 36°N latitude of the SGP site. There are some differences: both MMCR and RL report a minimum in the high-level clouds near 5PM. The MMCR reports a thinner extent of boundary layer clouds (up to 2.5km at most), while findings from the RL are more consistent with those from CATS. The MMCR reports almost no low-level clouds between 6PM and 6AM, while CATS and the RL report some clouds in that time frame -- they might be optically thin and missed by the radar. The RL reports almost none of the daytime PBL clouds so conspicuous in MMCR and CATS observations, perhaps because fully attenuating clouds were removed from the RL dataset for the Dupont et al. (2011) study as they hide most of the atmosphere from a ground-based lidar (unlike a spaceborne one).¶
 These deviations

Deleted: appear

Deleted: to us

Deleted:)

Deleted: the

Deleted: included in the MMCR and RL datasets (14 and 10 seasons)

Deleted: . M

Deleted: , CATS provides a correct

Deleted: of the diurnal evolution of the altitude of

Deleted: (not the occurrence in late afternoon)

Deleted: ¶

Deleted: using

Deleted: as a reference,

Deleted: seem to provide an interesting

Deleted: ation

Deleted: of

Deleted: validation

Deleted: certain regions:

Deleted: c

Deleted:

875 compared to single-site ground-based observations. Figure 5 illustrates how the diurnal
876 cycle of CF varies among seven large continental areas across both hemispheres, considering
877 only cloud detections made by CATS over land within lat-lon boxes (defined in the inset map)
878 during the summer seasons (JJA in the NH, DJF in the SH).

879 During summer most continents share a development of PBL clouds during sunlit hours
880 (with similar Cloud Fractions, hours and vertical extents), except NH Africa where low clouds
881 are almost absent. Most continents also share a nighttime maximum and daytime maximum
882 of high clouds, with an associated narrowing of their vertical distribution during morning
883 and a spreading out during the afternoon. Variations in cloudiness and cloud vertical
884 distribution are particularly intense over South America and SH Africa, while they are
885 minimal over Australia. A mid-altitude cloud layer is present almost all day long, with a faint
886 daytime minimum, over all SH continents and NH Africa.

887 Note that the present comparison is less robust in the lower troposphere than higher in the
888 troposphere, due to the attenuation of the space lidar signal as it penetrates the
889 atmosphere.

890

Deleted: thinning

Deleted: thickening

Deleted:

Deleted: thickness

895 **4. Discussion**

896

897 Hereafter we use our results for answering the following questions: How does the diurnal
898 cycle of low, mid, high cloud covers from geostationary satellites compare with CATS ones?

899 Do the existing lidar space missions document extreme or average behaviors of the cloud
900 profile diurnal cycle? What about upcoming sun-synchronous lidar space missions?

901

902 **4.1 About the Diurnal cycles of Low and High Cloud Amounts**

903

904 CATS observations provide an opportunity to compare the cloud diurnal cycle derived from
905 the ISCCP dataset (Sect. 2.1.c) with completely independent observations at near-global

906 scale (excluding latitudes higher than 51°). In particular, we expect cloud retrievals from an
907 active sensor such as CATS to be independent of the surface, even above highly reflective

908 surfaces, such as ice and deserts and to include optically thin clouds. Since CATS sampling is
909 constrained between 51°S and 51°N, its data cannot be used to document the diurnal cycle
910 in the polar regions, like ISCCP does: our comparison will extend at most to midlatitudes.

911 Figure 6 shows the diurnal cycle of the Low and High cloud covers observed by the CATS
912 space lidar.

913 Over ocean CAs are very stable, the diurnal cycle is almost flat (Fig. 6, left column). CATS
914 shows a weak cycle for low clouds, with a maximum in mid-morning and a minimum in
915 early-afternoon, which is also visible in ISCCP data. For oceanic high clouds, CATS exhibit
916 almost no diurnal cycle except in the Tropics where they follow the same cycle as low
917 clouds. ISCCP also shows a weak cycle for high clouds, but opposite to the CATS one. This
918 might be related to the fact that CATS can detect optically thin high clouds better than
919 ISCCP. The optically thicker high clouds seen by ISCCP are thus probably more linked to deep
920 convection activity. CATS can better detect optical thin high clouds, which should be more
921 decoupled from convection and less affected by diurnal cycles.

922 Over land, between 15°S and 51°N, CATS reports that low-clouds have a pronounced diurnal
923 cycle with a maximum of low-level clouds at midday (+10%) and a minimum at midnight (-
924 5%). This is consistent with ISCCP observations (Figure 11 in RS99), but in the Northern mid-

Deleted: u

Deleted: first

Deleted: technique (

Deleted:)

Deleted: contrarily to the passive remote sensing observations (ISCCP) that may sometimes confound clouds and surface over reflective surfaces

Deleted: . Moreover, CATS is expected

Deleted: observe

Deleted: more

Deleted: than passive sensors thanks to a lidar high sensitivity

Deleted: ¶

Deleted: , plotted in a similar way as Figure 11 in RS99 for easier comparison

Deleted: 60

941 latitudes the amplitude of the cycle is weaker for CATS than ISCCP (minimum at -4% instead
942 of -12%). For high-level clouds over land in the Tropics (15°S-30°N) CATS observes a
943 maximum during night-time and a minimum at noon; the timing is consistent with ISCCP but
944 the amplitude is slightly more pronounced with CATS than ISCCP (-12% instead of -7% at
945 midday). In the Southern hemisphere (15°S-51°S) the similarity between CATS and ISCCP
946 gets lost, probably because the land surface is small in those latitude ranges and the
947 observations are not significant.

Deleted: 60

948 In summary, CATS confirms the shape of the Low and High cloud diurnal cycles observed by
949 ISCCP except for high tropical clouds. This could be due to the space lidar detecting a larger
950 number of optically thinner clouds not directly linked to deep convection, or to the different
951 day-night cloud detection sensitivities of active and passive measurements. In most cases,
952 the amplitudes of the diurnal cycle observed by CATS differ from those observed by ISCCP.

Deleted: , likely

Deleted: because

Deleted: can

Deleted: more

Deleted: that are

953 Both CATS and ISCCP miss some low clouds that are masked by the presence of high thick
954 clouds. So even if CATS and ISCCP diurnal cycles are roughly consistent in low clouds, both
955 results might be biased in the same direction. The high clouds diurnal cycle presented here
956 are more robust than the low clouds ones.

957

958 **4.2 About the Cloud Fraction profiles observed at fixed local times by space lidars**

959 The CALIOP lidar has provided detailed Cloud Fraction profiles since 2006 at 0130AM and
960 0130 PM LT. The next spaceborne atmospheric lidar missions ADM-Aeolus, to be launched
961 in late 2018 (Culoma et al., 2017) on a sun-synchronous orbit, will enable measurements at
962 0600AM and 0600PM LT. After that, the ATLID lidar on the Earth-CARE platform (Illingworth
963 et al., 2015), expected to launch in 2020, will operate at fixed local times close to CALIOP
964 (02:00AM and PM). The CATS dataset may remain for the near future our single source of
965 diurnally distributed cloud profile lidar measurements from space.

966

967 *a) Comparison between CATS and CALIPSO*

968 In this section, we first check how CATS sees the day/night variation in cloud profiles also
969 documented by CALIOP through its two daily overpasses. Figure 7 shows vertical profiles of

976 Cloud Fraction reported by both datasets at 0130AM and PM, over ocean (left) and land
977 (right), latitude-weighted and averaged between 51°S and 51°N over JJA between 2015 and
978 2017. The black lines show the CF obtained when considering all measurements from both
979 instruments. Over land and ocean, we find that both CALIPSO and CATS overall report larger
980 Cloud Fractions at 0130AM (blue) than 0130PM (red), in agreement with the findings of
981 Gupta et al. (2018). Below 2.5 km, this difference is stronger over ocean (+7% in 0130AM
982 CF) than over land. Both datasets report a strong increase in 0130AM CF (almost +7%
983 compared to 0130PM) above 15km over land.

984 The CF profiles reported by both datasets agree very well over Ocean (left) in both daytime
985 and nighttime conditions. Over land (right) in daytime (red) conditions, CATS reports slightly
986 more low-level clouds (CF~7% near 1km ASL, ~5% for CALIOP). This difference, which is
987 present at all latitudes above land during daytime (not shown), might be due to the so-
988 called single-shot low clouds, for which CALIOP data undergoes a specific processing
989 (Winker et al., 2009). The strongest differences appear for nighttime CF over land (right,
990 blue): CALIPSO CF is larger than CATS CF by a 2-3% throughout the entire profile. A perfect
991 agreement between CF from both datasets should not be expected, as the CATS and CALIOP
992 lidars operate in different configurations – wavelengths, pulse repetition frequencies and
993 signal-to-noise ratios are different, for a start. These technical variations lead to differences
994 in, for instance, how fast the laser pulse energy of both instruments gets attenuated as it
995 penetrates atmospheres of various compositions, or differences in cloud detection
996 performance, e.g. when sampling optically thin clouds in the upper troposphere, or
997 fractionated boundary layer clouds (see Reverdy et al., 2015 for a study of the impact of
998 design choices on lidar retrievals). Both datasets agree quite well on the general vertical
999 pattern of the profile, though. A useful conclusion is that considering CALIPSO observations
1000 at both overpass local times (i.e. 0130AM and 0130PM) apparently provides a good
1001 approximation of the daily average Cloud Fraction profile.

1002

1003 b) Comparison of Cloud Fraction profiles at various times of satellite overpass

1004 As a final analysis, we represent the range covered by CATS hourly CF profiles over a day
1005 (averaged over the globe - white envelope in Fig. 8) and show CF profiles observed by CATS
1006 ±1 hour around the fixed local observation times of the three sun-synchronous space lidar

Deleted: C

Deleted: F

Deleted: c

Deleted: f

Deleted: Cloud Fraction

1012 missions (CALIPSO, ADM-Aeolus, EarthCare).

1013 Our first aim is to understand how wind observations made at fixed local time by ADM-
1014 Aeolus might be impacted by the cloud diurnal cycle. ADM-Aeolus will provide information
1015 on wind only in absence of clouds. Figure 8 indicates that ADM-Aeolus overpass times are
1016 quite cloudy in both AM and PM compared to the diurnal variability (white envelope). The
1017 PM overpass corresponds to the daily maximum in cloud profiles over both ocean and land,
1018 while AM observations correspond to a time representative of the daily average Cloud
1019 Fraction profile. As more clouds occur in the PM than AM observations, less wind
1020 information will likely be provided by ADM-Aeolus in the afternoon than in the morning. For
1021 the future, another ADM-Aeolus-like mission around midday (minimum Cloud Fraction
1022 profile) would increase the number of wind measurement with respect to the cloud
1023 occurrence.

1024 Our second aim is to understand how well observations made at fixed local times by space
1025 lidar dedicated to clouds studies (CALIPSO and EarthCare) capture the daily variability of
1026 Cloud Fraction profiles. Figure 8 suggests that over land (right), CALIPSO and Earth-CARE
1027 retrievals capture only part of the daily CF variability above 8km ASL: the PM measurements
1028 overestimate the daily CF minima and the AM measurements underestimate the daily CF
1029 maxima. Below 8km ASL they are rather representative of the daily average, except below
1030 5km ASL where PM measurements get close to the daily CF maxima. Figure 8 also shows
1031 that over Ocean (left) CALIPSO and Earth-CARE retrievals should be considered as the daily
1032 CF maxima during the nighttime (AM) overpass and as the daily CF minima during the
1033 daytime (PM) overpass. This has interesting implications: it suggests that not only CALIPSO
1034 but all the observations dedicated to cloud studies collected by the instruments within the
1035 A-train (CloudSat, CERES, MODIS, PARASOL, etc.) have documented the state of the
1036 atmosphere in the extreme states of the cloud profile diurnal cycle over the last 12 years
1037 over ocean. These conclusions suggest the A-Train observations are likely relevant and
1038 robust to constrain the cloud diurnal cycle extremes in climate models and climate studies.

1039

1040

Deleted: c

Deleted: f

Deleted: c

Deleted: f

Deleted: c

Deleted: f

1047 **5. Conclusions**

1048 In this paper, we took advantage of the variable local time of overpass of the International
1049 Space Station to document the diurnal cycle of the cloud vertical profile as seen by the CATS
1050 lidar. This is the first time the diurnal evolution of the vertical cloud profile is documented on
1051 that vertical scale on a large part of the globe, between 51°S and 51°N. Our results are based
1052 on 15 months of systematic observations (3 boreal summers and 2 austral summers)
1053 collected during the 2015-2017 time period, which enable statistically significant results.

1054 The main results follow. We observed that high tropical clouds begin to spread out vertically
1055 in the late afternoon (4-5PM). Their vertical distribution is largest (over 5km) near 10PM.
1056 This spread-out is particularly large in the Summer Hemisphere in DJF. A mid-level cloud
1057 layer (4-8 km ASL) persists all day long over the tropical continent during summer, with a
1058 weak diurnal cycle (minimum at noon). Southern Ocean results are quite unique; low clouds
1059 (0-2km ASL) cover this ocean all day long in summer and winter. A slight diurnal cycle sees
1060 their CF drop by a few percents during the afternoon (from noon to 6PM), but their vertical
1061 distribution stays constant. High clouds are also frequent over the Southern Ocean, more so
1062 in JJA. They follow a diurnal cycle in summer and winter, with a daytime minimum (from
1063 8AM and 3PM). At all latitudes, continental low clouds are most frequent in the early
1064 afternoon (around 2PM) at about 2.5 km ASL. Finally, our results show that in summer the
1065 diurnal cycle of continental clouds is similar in both hemispheres: a rapid development of
1066 near-surface PBL clouds during sunlit hours, and an increase in cloudiness and wider vertical
1067 distributions during nighttime for high-altitude clouds (stronger over the SH and the
1068 Tropics). Exceptions are NH Africa, where PBL clouds are very few, and Australia, where high
1069 clouds appear only significant between 8 and 11PM.

1070 We evaluated the diurnal cycle derived from CATS against independent ground-based
1071 observations and found satisfactory agreement. Moreover, our results suggest that over
1072 oceans, CALIPSO and Earth-CARE should describe the daily minimum of the Cloud Fraction
1073 profile during their PM overpass, and its daily maximum during their AM overpass. This
1074 supports the idea that data collected by A-train instruments (not only CALIPSO) are very
1075 relevant to document the cloud diurnal cycle. This is also roughly the case over land at
1076 altitudes above 8km ASL, although the amplitude of the diurnal variability is quite

- Deleted: ¶
- Deleted: ¶
- Deleted: are the following
- Deleted: the
- Deleted: start getting
- Deleted: thicker late
- Deleted: and reach their maximum thickness of 4-
- Deleted: near 10PM
- Deleted: thickening
- Deleted: intense
- Deleted: Our results reveal a
- Deleted: ent
- Deleted: this ocean is covered by
- Deleted: thickness stays
- Deleted: ,
- Deleted: and
- Deleted: all year long
- Deleted: n
- Deleted: earlier
- Deleted: early morning to early afternoon
- Deleted: O
- Deleted: also
- Deleted: the diurnal cycle of
- Deleted: in summer share similar features
- Deleted: over continents
- Deleted: the
- Deleted: cloud thickness
- Deleted: at
- Deleted:
- Deleted: s
- Deleted: during nighttime
- Deleted: rare
- Deleted: we discussed the implications of our results for... [3]
- Deleted: cloud profiles from
- Deleted: over oceans
- Deleted: nearly
- Deleted: c
- Deleted: f
- Deleted: vertical
- Deleted: ,
- Deleted: which
- Deleted: all

1123 underestimated.

1124 Questions remain about how several factors could affect our ability to retrieve the vertical
1125 variability of clouds from lidar-based measurements through the day. More specifically, the
1126 irruption of solar noise in daytime conditions requires increased horizontal averaging to
1127 keep CATS detection sensitivity stable. High clouds with very small optical depths (lower
1128 than 0.005), which CATS can detect in the nighttime, will be probably missed in the daytime.
1129 Meanwhile, the occurrence and extent of fragmented boundary layer clouds might be
1130 overestimated. Even though prior work using the similarly-affected CALIPSO data suggests
1131 the observed diurnal changes in clouds are too large to be solely due to those effects, their
1132 impact on the retrieved cycles needs to be quantified. In the same manner, how extinction
1133 by high clouds impacts the retrieved Cloud Fractions at low altitude needs to be
1134 investigated.

1135 In the future, it would be possible to consider CATS measurements at smaller scales, to
1136 identify regionally consistent cloud populations and diurnal behaviors over specific regions
1137 of interest. It would also be possible to use CATS detection of opaque cloud layers to identify
1138 the best local time of observation from space to study local cloud radiative effects. We will
1139 address these lines of research in upcoming papers.

1140 Acknowledgments

1141 CATS and CALIPSO data were obtained through the NASA Langley Research Atmospheric
1142 Science Data Center (ASDC) and the AERIS and ICARE/CGTD Data services. ARM-ENA and
1143 ARM-SGP data were obtained through the ARM portal at <http://www.arm.gov>, SIRTA data
1144 were obtained through the ReOBS portal at <http://sirta.ipsl.fr/reobs.html>. Data were
1145 analyzed on the Climserv IPSL computing facilities. This research was made possible through
1146 support by CNRS and CNES. We want to thank J.-L. Baray and N. Montoux for useful
1147 discussions.

Deleted: hope to

Formatted: Heading 1, Justified, Line spacing: 1,5 lines

Deleted: CALIPSO and CloudSat datasets were provided by

Deleted: through

Deleted: ¶
¶

1153 **References**

1154

1155 • Ackerman, T. P., and G. M. Stokes (2003), The Atmospheric Radiation Measurement
1156 Program Phys. Today, 56, 38–44, doi:10.1063/1.1554135

1157 • Bouniol, D., R. Roca, T. Fiolleau, and D.E. Poan, 2016: [Macrophysical, Microphysical,
1158 and Radiative Properties of Tropical Mesoscale Convective Systems over Their Life
1159 Cycle](#). *J. Climate*, **29**, 3353–3371, doi:10.1175/JCLI-D-15-0551.1

1160 • Bourgeois, E., D. Bouniol, F. Couvreux, F. Guichard, J. H. Marsham, L. Garcia-Carreras,
1161 C. E. Birch, and D. J. Parker (2018), Characteristics of mid-level clouds over West
1162 Africa, *QJRMS*, **113**, D04210–17, doi:10.1002/qj.3215.

1163 • Ceppi, P., F. Brient, M. D. Zelinka, and D. L. Hartmann, 2017: Cloud feedback
1164 mechanisms and their representation in global climate models, *WIREs Climate
1165 Change* 2017, e465. Doi: 10.1002/wcc.465

1166 • Cesana, G., and H. Chepfer (2013), Evaluation of the cloud thermodynamic phase in a
1167 climate model using CALIPSO-GOCCP, *J. Geophys. Res.*, **118**(14), 7922–7937,
1168 doi:10.1002/jgrd.50376.

1169 • Cesana, G., H. Chepfer, D.M. Winker, B. Getzewich, X. Cai, H. Okamoto, Y. Hagihara, O.
1170 Jourdan, G. Mioche, V. Noel, M. Reverdy, 2016: Using in situ airborne measurements
1171 to evaluate three cloud phase products derived from CALIPSO, *J. Geophys. Res.*
1172 *Atmos.*, **121**, 5788–5808, doi:10.1002/2015JD024334

1173 • Chepfer, H., Bony, S., Winker, D., Cesana, G., Dufresne, J. L., Minnis, P., Stubenrauch,
1174 C. J. and Zeng, S.: The GCM-Oriented CALIPSO Cloud Product (CALIPSO-GOCCP), *J.*
1175 *Geophys. Res.*, **115**(1), 23073–13, doi:10.1029/2009JD012251, 2010.

1176 • Chepfer H., G. Cesana, D. Winker, B. Getzewich, and M. Vaughan, 2013: Comparison
1177 of two different cloud climatologies derived from CALIOP Level 1 observations: the
1178 CALIPSO-ST and the CALIPSO-GOCCP, *J. Atmos. Ocean. Tech.*, doi.10.1175/JTECH-D-
1179 12-00057.1

1180 • Chiriaco M., S. Bastin, P. Yiou, M. Haeffelin, J.-C. Dupont, L. Klenov, M. Stéfanon,
1181 2014: European heat-wave in July 2006: observations and modelling showing how

Formatted: English (US)

Formatted: English (US)

Formatted: English (US)

Formatted: English (UK)

Formatted: English (US)

Formatted: Indent: Hanging: 0,88 cm

Formatted: English (US)

Deleted: <#>¶

1183 local processes amplify conducive large-scale conditions. *Geophys. Res. Lett.*, 41 issue
1184 15, 5644 – 5652.

- 1185 • [Chiriaco, M., Dupont, J.-C., Bastin, S., Badosa, J., Lopez, J., Haeffelin, M., Chepfer, H.,](#)
1186 [and Guzman, R.: ReOBS: a new approach to synthesize long-term multi-variable](#)
1187 [dataset and application to the SIRTA supersite, *Earth Syst. Sci. Data*, 10, 919-940,](#)
1188 <https://doi.org/10.5194/essd-10-919-2018>, 2018
- 1189 • [Culoma A., A. Elfving, R. Meynart, A. Straume, D. Wernham, "AEOLUS mission: the](#)
1190 [latest preparations before launch", *Proc. SPIE 10423, Sensors, Systems, and Next-*](#)
1191 [Generation Satellites XXI, 1042303 \(29 September 2017\); doi: 10.1117/12.2282159](#)
- 1192 • [Dong, X., B. Xi, K. Crosby, C. N. Long, R. S. Stone, and M. D. Shupe \(2010\), A 10 year](#)
1193 [climatology of Arctic cloud fraction and radiative forcing at Barrow, Alaska, *J.*](#)
1194 [Geophys. Res.](#), 115(D17), D17212, doi:10.1029/2009JD013489.
- 1195 • Dupont, J. C., M. Haeffelin, Y. Morille, V. Noel, P. Keckhut, D. Winker, J. Comstock, P.
1196 Chervet, and A. Roblin (2010), Macrophysical and optical properties of midlatitude
1197 cirrus clouds from four ground-based lidars and collocated CALIOP observations, *J.*
1198 *Geophys. Res.*, 115(D4), D00H24–15, doi:10.1029/2009JD011943.
- 1199 • Elouragini, S. and Flamant, P. H.: Iterative method to determine an averaged lidar
1200 ratio and the range resolved extinction in cirrus, *Appl. Opt.*, 35, 1512–1518, 1996.
- 1201 • [Gray, W. M., and R. W. Jacobson, 1977: Diurnal variation of deep cumulus convection.](#)
1202 [Mon. Wea. Rev.](#), 105, 1171–1188, doi:10.1175/1520-
1203 [0493\(1977\)105,1171:DVODCC.2.0.CO;2](#)
- 1204 • [Greenwald, T. J. and Christopher, S. A.: Daytime variation of marine stratocumulus](#)
1205 [microphysical properties as observed from geostationary satellite, *Geophysical*](#)
1206 [Research Letters](#), 26(1), 1723–1726, doi:10.1029/1999GL900346, 1999.
- 1207 • Guzman, R., H. Chepfer, V. Noel, T. Vaillant de Guélis, J. E. Kay, P. Raberanto, G.
1208 Cesana, M. A. Vaughan, and D. M. Winker (2017), Direct atmosphere opacity
1209 observations from CALIPSO provide new constraints on cloud-radiation interactions,
1210 *J. Geophys. Res.*, 1–20, doi:10.1002/2016JD025946.
- 1211 • Haeffelin, M. et al. (2005), SIRTA, a ground-based atmospheric observatory for cloud

Formatted: English (US)

Deleted: <#>Chiriaco, M., Dupont, J.-C., Bastin, S., Badosa, J., Lopez, J., Haeffelin, M., Chepfer, H., and Guzman, R.: ReOBS: a new approach to synthesize long-term multi-variable dataset and application to the SIRTA supersite, *Earth Syst. Sci. Data Discuss.*, <https://doi.org/10.5194/essd-2017-101>, in review.¶

1218 and aerosol research, *Annales Geophysicae*, 23(2), 253–275, doi:10.5194/angeo-23-
1219 253-2005.

1220 • Haynes, J. M., T. H. Vonder Haar, T. L'Ecuyer and D. Henderson (2013) Radiative
1221 heating characteristics of earth's cloudy atmosphere from vertically resolved active
1222 sensors. *Geophys Res Lett* 40:624–904 630. doi:10.1002/grl.50145.

Formatted: English (US)

1223 • Hoareau, C., P. Keckhut, V. Noel, H. Chepfer, and J. L. Baray (2013), A decadal cirrus
1224 clouds climatology from ground-based and spaceborne lidars above the south of
1225 France (43.9° N–5.7° E), *Atmos. Chem. Phys.*, 13(14), 6951–6963, doi:10.5194/acp-
1226 13-6951-2013.

1227 • Hogan, R. J., A. J. Illingworth, E. J. O'Connor, and J. P. V. Poiars Baptista (2003),
1228 Characteristics of mixed-phase clouds. II: A climatology from ground-based lidar,
1229 *QJRMMS*, 129, 2117–2134.

Formatted: English (US)

1230 • Hu, Y. et al. (2009), CALIPSO/CALIOP Cloud Phase Discrimination Algorithm, *J. Atmos.*
1231 *Oceanic Technol.*, 26, 2293–2309.

1232 • Illingworth, A. J. et al. (2015), The EarthCARE Satellite: The Next Step Forward in
1233 Global Measurements of Clouds, Aerosols, Precipitation, and Radiation, *Bull. Am.*
1234 *Met. Soc.*, 96(8), 1311–1332, doi:10.1175/BAMS-D-12-00227.1.

1235 • Johnson, R. H., T. M. Rickenbach, S. A. Rutledge, P. E. Ciesielski, and W. H. Schubert
1236 (1999), Trimodal Characteristics of Tropical Convection, *J. Climate*, 12(8), 2397–2418,
1237 doi:10.1175/1520-0442(1999)012<2397:TCOTC>2.0.CO;2.

1238 • Kato, S., F. G. Rose, S. S. Mack, W. F. Miller, and co-authors (2011), Improvements of
1239 top-of-atmosphere and surface irradiance computations with CALIPSO-, CloudSat-,
1240 and MODIS-derived cloud and aerosol properties. *J Geophys Res* 116:D19209.
1241 doi:10.1029/2011JD016050

1242 • Kollias, P., Bharadwaj, N., Widener, K., Jo, I. and Johnson, K.: Scanning ARM Cloud
1243 Radars. Part I: Operational Sampling Strategies, *J. Atmos. Oceanic Technol.*, 31(3),
1244 569–582, doi:10.1175/JTECH-D-13-00044.1, 2014.

1245 • Konsta, D., J. L. Dufresne, H. Chepfer, A. Idelkadi, and G. Cesana (2016), Use of A-train
1246 satellite observations (CALIPSO–PARASOL) to evaluate tropical cloud properties in the

1247 LMDZ5 GCM, *Clim. Dyn.*, 1–22, doi:10.1007/s00382-015-2900-y.

1248 • Kummerow, C., W. Barnes, T. Kozu, J. Shiue, and J. Simpson (1998), The Tropical
 1249 Rainfall Measuring Mission (TRMM) sensor package, *J. Atmos. Oceanic Technol.*, 15,
 1250 809–817.

1251 • L'Ecuyer, T. S., N. B. Wood, T. Haladay, G. L. Stephens, and P. W. Stackhouse
 1252 Jr. (2008), Impact of clouds on atmospheric heating based on the R04 CloudSat fluxes
 1253 and heating rates data set, *J. Geophys. Res.*, 113, D00A15,
 1254 doi:[10.1029/2008JD009951](https://doi.org/10.1029/2008JD009951).

1255 • L'Ecuyer, T. S., and J. H. Jiang, 2010: Touring the atmosphere aboard the A-Train.
 1256 *Physics Today*, vol .63 (7), 36-40.

1257 • [Liu, Z., M. A. Vaughan, D. Winker, C. Kittaka, B. Getzewich, R. Kuehn, A. Omar, K. A.
 1258 Powell, C. Trepte, and C. Hostetler \(2009\), The CALIPSO lidar cloud and aerosol
 1259 discrimination: Version 2 algorithm and initial assessment of performance, *J. Atmos.
 1260 Oceanic Technol.*, 26, 1198–1213.](#)

1261 • [Masunaga, H., T.S. L'Ecuyer, and C.D. Kummerow, 2005: Variability in the
 1262 Characteristics of Precipitation Systems in the Tropical Pacific. Part I: Spatial
 1263 Structure. *J. Climate*, 18, 823–840, <https://doi.org/10.1175/JCLI-3304.1>.](#)

1264 • McGill, M. J., J. E. Yorks, V. S. Scott, A. W. Kupchock, and P. A. Selmer (2015), The
 1265 Cloud-Aerosol Transport System (CATS): A technology demonstration on the
 1266 International Space Station, Proc. SPIE 9612, Lidar Remote Sensing for Environmental
 1267 Monitoring XV, 96120A, doi:10.1117/12.2190841.

1268 • [Naud, C., Del Genio, A. D., Haeffelin, M., Morille, Y., Noel, V., Dupont, J.-C., Turner, D.,
 1269 Lo, C., and Comstock, J. M., 2010: Thermodynamic phase profiles of optically thin
 1270 midlatitude clouds and their relation to temperature. *J. Geophys. Res.*, 115 D11202](#)

1271 • [Noel, V. and Haeffelin, M., 2007: Midlatitude Cirrus Clouds and Multiple Tropopauses
 1272 from a 2002-2006 Climatology over the SARTA observatory. *J. Geophys. Res.*, 112
 1273 D13206](#)

1274 • [Wang, Z., and K. Sassen, 2001: Cloud type and macrophysical property retrieval using
 1275 multiple remote sensors. *J. Appl. Meteor.*, 40, 1665-1682](#)

Formatted: English (US)

Field Code Changed

Formatted: English (US)

Formatted: English (US)

Field Code Changed

Formatted: English (US)

Formatted: English (US)

Deleted: Moran, K. P., B. E. Martner, M. J. Post, R. A. Kropfli, D. C. Welsh, and K. B. Widener (1998), An unattended cloud-profiling radar for use in climate research, *Bull. Am. Meteorol. Soc.*, 79, 443–455.

Formatted: English (US)

Formatted: English (US)

Formatted: Font: Not Italic

- 1280 • Palm, S. P., D. L. Hlavka, P. Selmer, R. Pauly, 2016: the Cloud Aerosol Transport System
1281 (CATS) Data Product Catalog release 3.0. Retrieved on January 23rd 2018 from
1282 https://cats.gsfc.nasa.gov/media/docs/CATS_Data_Products_Catalog.pdf
- 1283 • Pappalardo, G., Amodeo, A., Apituley, A., Comeron, A., Freudenthaler, V., Linné, H.,
1284 Ansmann, A., Bösenberg, J., D'Amico, G., Mattis, I., Mona, L., Wandinger, U., Amiridis,
1285 V., Alados-Arboledas, L., Nicolae, D., and Wiegner, M.: EARLINET: towards an
1286 advanced sustainable European aerosol lidar network, *Atmos. Meas. Tech.*, 7, 2389-
1287 2409, doi:10.5194/amt-7-2389-2014, 2014
- 1288 • [Philippon, N. et al. \(2016\), Analysis of the diurnal cycles for a better understanding of
1289 the mean annual cycle of forests greenness in Central Africa, *Agricultural and Forest
1290 Meteorology*, 223, 81–94, doi:10.1016/j.agrformet.2016.04.005.](#)
- 1291 • [Protat, A., J. Delanoë, A. Plana-Fattori, P. T. May, and E. J. O'Connor \(2009\), The
1292 statistical properties of tropical ice clouds generated by the West African and
1293 Australian monsoons, from ground-based radar-lidar observations, *QJRM*, 136\(S1\),
1294 345–363, doi:10.1002/qj.490.](#)
- 1295 • Reverdy, M., Noel, V., Chepfer, H., & Legras, B. (2012). On the origin of subvisible
1296 cirrus clouds in the tropical upper troposphere. *Atmospheric Chemistry and Physics*,
1297 12(24), 12081–12101. <http://doi.org/10.5194/acp-12-12081-2012>
- 1298 • [Reverdy, M., H. Chepfer, D. Donovan, V. Noel, G. Cesana, C. Hoareau, M. Chiriaco, and
1299 S. Bastin \(2015\), An EarthCARE/ATLID simulator to evaluate cloud description in
1300 climate models, *J. Geophys. Res.*, 120\(2\), 11, doi:10.1002/2015JD023919.](#)
- 1301 • [Rossow, W. B., 1989: Measuring cloud properties from space: A review. *J. Climate*, 2,
1302 201–213](#)
- 1303 • [Rozendaal, M. A., Leovy, C. B., and Klein, S. A.: An Observational Study of Diurnal
1304 Variations of Marine Stratiform Cloud, *J. Climate*, 8, 1795–1809, 1995.](#)
- 1305 • [Sassen, K., and S. Benson \(2001\), A midlatitude Cirrus Cloud Climatology from the
1306 Facility for Atmospheric Remote Sensing. Part II : microphysical properties derived
1307 from lidar depolarisation, *J. Atmos. Sci.*, 58, 2103–2112, doi:10.1175/1520-
1308 0469\(2001\)058<2103:AMCCCF>2.0.CO;2.](#)

Formatted: English (UK)

Formatted: English (UK)

1309 • Sassen, K., Z. Wang, and D. Liu (2009), Cirrus clouds and deep convection in the
 1310 tropics: Insights from CALIPSO and CloudSat, *J. Geophys. Res.*, 114, D00H06,
 1311 doi: 10.1029/2009JD011916.

1312 • Sassen, K., and Z. Wang (2012), The Clouds of the Middle Troposphere: Composition,
 1313 Radiative Impact, and Global Distribution, *Surveys in Geophysics*, 33(3-4), 677–691,
 1314 doi:10.1007/s10712-011-9163-x.

1315 • Sèze, G., J. Pelon, M. Derrien, H. Le Gléau, and B. Six (2014), Evaluation against
 1316 CALIPSO lidar observations of the multi-geostationary cloud cover and type dataset
 1317 assembled in the framework of the Megha-Tropiques mission, *QJRM*, 141(688),
 1318 774–797, doi:10.1002/qj.2392.

1319 • Shang, H., H. Letu, T. Y. Nakajima, Z. Wang, R. Ma, T. Wang, Y. Lei, D. Ji, S. Li, and J. Shi
 1320 (2018), Diurnal cycle and seasonal variation of cloud cover over the Tibetan Plateau
 1321 as determined from Himawari-8 new-generation geostationary satellite data,
 1322 *Scientific Reports*, 1–8, doi:10.1038/s41598-018-19431-w.

1323 • Soden, B. J. (2000), The diurnal cycle of convection, clouds, and water vapor in the
 1324 tropical upper troposphere. *Geophys. Res. Lett.* 27 (15), 2173-2176. doi:
 1325 10.1029/2000GL011436

1326 • Stephens, G. L., & Kummerow, C. D. (2007). The Remote Sensing of Clouds and
 1327 Precipitation from Space: A Review. *Journal of the Atmospheric Sciences*, 64(11),
 1328 3742–3765. <http://doi.org/10.1175/2006JAS2375.1>

1329 • Stephens, G., D. Winker, J. Pelon, C. Trepte, D. Vane, C. Yuhas, T. L'Ecuyer, and M.
 1330 Lebsock, 2018: CloudSat and CALIPSO within the A-Train: Ten Years of Actively
 1331 Observing the Earth System, *Bull. Amer. Meteor. Soc.*, 99, 569–
 1332 581, <https://doi.org/10.1175/BAMS-D-16-0324.1>

1333 • Stubenrauch, C.J., A. Chédin, G. Rädcl, N.A. Scott, and S. Serrar, 2006: Cloud
 1334 Properties and Their Seasonal and Diurnal Variability from TOVS Path-B. *J. Climate*,
 1335 19, 5531–5553, <https://doi.org/10.1175/JCLI3929.1>

1336 • Taylor, S., Stier, P., White, B., Finkensieper, S., and Stengel, M.: Evaluating the diurnal
 1337 cycle in cloud top temperature from SEVIRI, *Atmos. Chem. Phys.*, 17, 7035-7053.

Formatted: English (US)

Formatted: French

Formatted: English (UK)

Formatted: English (UK)

Formatted: English (US)

Field Code Changed

Formatted: English (US)

Formatted: English (US)

Deleted: Stephens, G., D. Winker, J. Pelon, C. Trepte, D. Vane, C. Yuhas, T. L'Ecuyer, and M. Lebsock, 2017: CloudSat and CALIPSO within the A-Train: Ten years of actively observing the Earth system. *Bull. Amer. Meteor. Soc.* doi:10.1175/BAMS-D-16-0324.1, in press.

- 1343 <https://doi.org/10.5194/acp-17-7035-2017>, 2017
- 1344 • Vaughan, M. A., K. A. Powell, D. M. Winker, C. A. Hostetler, R. E. Kuehn, W. H. Hunt, B.
- 1345 J. Getzewich, S. A. Young, Z. Liu, and M. J. McGill (2009), Fully Automated Detection
- 1346 of Cloud and Aerosol Layers in the CALIPSO Lidar Measurements, *J. Atmos. Oceanic*
- 1347 *Technol.*, 26(10), 2034–2050, doi:10.1175/2009JTECHA1228.1.
- 1348 • [Wilson, A. M. and Barros, A. P.: Orographic Land–Atmosphere Interactions and the](#)
- 1349 [Diurnal Cycle of Low-Level Clouds and Fog, *J. Hydrometeor.*, 18\(5\), 1513–1533,](#)
- 1350 [doi:10.1175/JHM-D-16-0186.1, 2017.](#)
- 1351 • Winker, D., M. A. Vaughan, A. Omar, Y. Hu, and K. A. Powell (2009), Overview of the
- 1352 CALIPSO mission and CALIOP data processing algorithms, *J. Atmos. Oceanic Technol.*,
- 1353 26, 2310–2323.
- 1354 • Winker DM, Pelon J, Coakley JA Jr, Ackerman SA, Charlson RJ, Colarco PR, Flamant P,
- 1355 Fu Q, Hoff RM, Kittaka C, Kubar TL, Le Treut H, McCormick MP, Mé g ie G, Poole L,
- 1356 Powell K, Trepte C, Vaughan MA, Wielicki BA. 2010. The CALIPSO mission: A global 3D
- 1357 view of aerosols and clouds. *Bull. Am. Meteorol. Soc.* 91: 1211–1229.
- 1358 • Winker, D., Chepfer, H., Noel, V. and X. Cai. : Observational Constraints on Cloud
- 1359 Feedbacks: The Role of Active Satellite Sensors. *Surv in Geophys* (2017).
- 1360 Doi:10.1007/s10712-017-9452-0
- 1361 • Wylie, D. (2008), Diurnal Cycles of Clouds and How They Affect Polar-Orbiting
- 1362 Satellite Data, *J. Climate*, 21(16), 3989–3996, doi:10.1175/2007JCLI2027.1.
- 1363 • [Yin, J., & Porporato, A. \(2017\). Diurnal cloud cycle biases in climate models. *Nature*](#)
- 1364 [Communications, 8\(1\), 2269.](#)
- 1365 • [Yorks, J. E., D. L. Hlavka, W. D. Hart, M. J. McGill, 2011: Statistics of Cloud Optical](#)
- 1366 [Properties from Airborne Lidar Measurements. *J. Atmos. Oceanic Technol.*, 28, 869–](#)
- 1367 [883. doi: http://dx.doi.org/10.1175/2011JTECHA1507.1](#)
- 1368 • Yorks, J. E., M. J. McGill, S. P. Palm, D. L. Hlavka, P. A. Selmer, E. P. Nowotnick, M. A.
- 1369 Vaughan, S. D. Rodier, and W. D. Hart (2016a), An overview of the CATS level 1
- 1370 processing algorithms and data products, *Geophys. Res. Lett.*, 43, 4632–4639,
- 1371 doi:[10.1002/2016GL068006](https://doi.org/10.1002/2016GL068006).

Formatted: English (UK)

Formatted: English (US)

Field Code Changed

- 1372 • Yorks, J. E., S. P. Palm, M. J. McGill, D. L. Hlavka, W. D. Hart, P. A. Selmer, E.
1373 Nowotnick (2016b), CATS Algorithm Theoretical Basis Document, Level 1 and Level 2
1374 Data Products, release 1.2. Retrieved on February 13th 2018 from
1375 https://cats.gsfc.nasa.gov/media/docs/CATS_ATBD.pdf
- 1376 • Yorks, J. E., S.D. Rodier, E. Nowotnick, P.A. Selmer, M.J. McGill, S.P. Palm, and M. A.
1377 Vaughan (2018), CATS Level 2 Vertical Feature Mask Algorithms and Data Products:
1378 An Overview and Initial Assessment, Atmos. Meas. Tech. Discuss., in preparation.
- 1379 • Zhao, W., R. Marchand, and Q. Fu (2017), The diurnal cycle of clouds and
1380 precipitation at the ARM SGP site: Cloud radar observations and simulations from the
1381 multiscale modeling framework, J. Geophys. Res., 122(14), 7519–7536,
1382 doi:10.1002/2016JD026353.

), while RL cloud detections are available since 1998 (Ackerman and Stokes, 2003).

.

In the framework of the present study we did no specific processing of data from these instruments. Instead, we compare CATS cloud retrievals over the SGP site with the descriptions made by Zhao et al. (2017, Fig. 3a) and Dupont et al. (2011, Fig. 3) of the diurnal cycle of clouds over SGP based on 14 years of MMCR cloud detections and 10 years of RL cloud detections in Sect. 3.3

.

we discussed the implications of our results for spaceborne instruments from sun-synchronous satellite missions (CALIPSO and the A-train, ADM, Earth-CARE). O